

Status of \mathbb{Z}_3 -NMSSM featuring a light bino-dominated LSP and a light singlet-like scalar under the LZ Experiment

Haijing Zhou, Guangning Ban

Physics Department, Henan Normal University, Xinxiang 453007, China

E-mail: zhouhaijing0622@163.com

ABSTRACT: In the presence of a light singlet-like scalar state, the Bino-dominated dark matter (DM) candidate in the \mathbb{Z}_3 -symmetric Next-to-Minimal Supersymmetric Standard Model (\mathbb{Z}_3 -NMSSM) exhibits significant differences from its counterpart in the Minimal Supersymmetric Standard Model (MSSM), both in terms of intrinsic properties and mechanisms governing DM relic density and detection. Motivated by recent advancements in particle physics experiments, we systematically analyzed the implications of these developments for the \mathbb{Z}_3 -NMSSM framework featuring a light bino-dominated DM candidate and a light singlet-like scalar, ensuring theoretical consistency with empirical observations. Of paramount relevance are the latest direct detection constraints from the LUX-ZEPLIN (LZ) experiment, supersymmetry (SUSY) searches at the Large Hadron Collider (LHC), and precision measurements of the Muon g-2 anomaly at Fermilab, which collectively impose complementary constraints on the model's parameter space. Our investigation utilized the MultiNest algorithm to perform a rigorous parameter space scan, informed by the LZ(2022) experimental limits, while incorporating constraints from LHC Higgs analyses, Muon g-2 data, and B-physics observables. The results demonstrate that current experimental bounds, particularly stringent limits on spin-independent (SI) and spin-dependent (SD) DM-nucleus scattering cross-sections, coupled with LHC exclusion limits on electroweakinos, strongly disfavor this scenario. Nonetheless, the model retains the capacity to naturally reproduce the Z boson mass and Standard Model-like Higgs boson mass, explain the Muon Anomalous Magnetic Moment, and generate substantial corrections to the W boson mass. These findings exclusively manifest within the NMSSM framework, arising from the interplay between bino-dominated DM and singlino components, mediated through indispensable higgsino participation.

Contents

1	Introduction	1
2	Next-to-minimal supersymmetric standard model	4
2.1	Fundamental NMSSM properties	4
2.2	Dark matter sector	7
3	Numerical Results	12
3.1	Research strategy	12
3.2	Dark Matter phenomenology	15
3.3	Collider constraints	18
4	Conclusion	22

1 Introduction

The discovery of the Higgs boson in 2012 at the Large Hadron Collider (LHC) [1, 2] confirmed the validity of the Higgs mechanism as the origin of subatomic particle masses. Over the subsequent decade, precision measurements encompassing the Higgs boson’s production cross-sections, decay channels, and couplings by the ATLAS and CMS collaborations have maintained consistency with Standard Model (SM) predictions within approximately 2σ confidence levels [3, 4]. However, several lines of evidence, both theoretical (such as the hierarchy problem and the lack of gauge coupling unification) and experimental (including neutrino masses and the matter-antimatter asymmetry), suggest that the SM may not be the ultimate description of Nature but rather should be considered a low-energy effective theory of a more fundamental framework yet to be discovered.

There exist several BSM theories that address these weaknesses of the SM while identifying the 125 GeV scalar particle as a part of an extended scalar sector. Among these, the most widely accepted frameworks are supersymmetry (SUSY) models with R-parity conservation, specifically the Minimal Supersymmetric Standard Model (MSSM) [5, 6] and the Next-to-Minimal Supersymmetric Standard Model (NMSSM) [7–10]. These models elegantly resolve the hierarchy problem by introducing contributions from superpartners to the Higgs mass term. In addition, R-parity conservation ensures the stability of the lightest neutralino if it is the lightest supersymmetric particle (LSP), making it a well-motivated dark matter (DM) candidate. The MSSM, as the most parsimonious realization of SUSY, exhibits compelling theoretical advantages, but also includes some challenges (e.g., the “ μ -problem” [11] and “little hierarchy problem” [12]) that have become exacerbated in recent years by the first run of the LHC experiments. This was particularly true for the

uncomfortably large mass of the discovered Higgs boson $m_h \simeq 125$ GeV [13–21]. Alternatively, the NMSSM solves the μ -problem through the introduction of a gauge singlet chiral superfield (\hat{S}), extending the MSSM superpotential to

$$W = \lambda S H_u H_d + \frac{\kappa}{3} S^3. \quad (1.1)$$

where the μ parameter becomes dynamically generated as $\mu_{\text{eff}} = \lambda v_s$ upon electroweak symmetry breaking. Here v_s denotes the vacuum expectation value (VEV) of \hat{S} , and the magnitude of μ_{eff} is naturally stabilized at the electroweak scale through dimensionless Yukawa couplings λ and κ [8, 9]. In the decoupling limit ($\lambda, \kappa \rightarrow 0$ and $v_s \rightarrow \infty$) [8], the NMSSM phenomenologically recovers to an MSSM-like framework.

The NMSSM Higgs sector features two additional CP-even (h_s) and CP-odd (a_s) singlet scalar states compared to the MSSM. Furthermore, the MSSM neutralino sector is extended by a singlet Majorana fermion – the ‘singlino’. Similar to the MSSM framework, the lightest neutralino in the NMSSM serves as a cold dark matter (DM) candidate in the form of weakly interacting massive particles (WIMPs)¹. The physical masses and compositional structure of the neutralinos are strongly influenced by mixing among different states, with profound implications for both DM phenomenology and collider observables.

Under stringent and improved upper bounds on SI and SD DM-nucleon scattering cross sections, the DM candidate in the MSSM is predominantly bino-dominated and co-annihilates with the wino-like electroweakinos (EWinos) to achieve the measured relic abundance [34]. In this context, the SD scattering cross section σ^{SD} depends solely on μ and is suppressed by a factor of $1/\mu^4$. Current LZ experiment constraint on σ^{SD} necessitate substantially large μ . As demonstrated in Refs. [35, 36], the LZ(2022) experiment alone imposes a lower bound on the higgsino mass, $\mu \gtrsim 380$ GeV. This bound can be enhanced by several tens of GeV after incorporating the radiative correction to the scattering [37, 38]. Although such elevated μ values may naturally emerge through the well-known Giudice–Masiero mechanism in the gravity-mediated SUSY breaking scenario [39], they induce acute fine-tuning challenges in the precision prediction of the Z boson mass, especially after considering the LHC Higgs discovery and the non-observation of any DM or supersymmetric particle signals in experiments as the theory evolves from an ultraviolet high-energy scale to the electroweak scale [40–42].

Due to the distinct configurations of the EWino and Higgs sectors, the LSP in the NMSSM can exhibits markedly different properties compared to the MSSM, both in its

¹Serving for a WIMP, DM might be detected by measuring DM-nucleon scattering. In the non-relativistic limit, only two different kinds of interactions between a neutralino and a nucleon need to be considered [22]: spin-dependent (SD) interaction where the WIMP couples to the spin of the nucleus, and spin-independent (SI) interaction where the WIMP couples to the mass of the nucleus. The WIMPs are theoretically predicted to couple with Standard Model (SM) particles via weak interactions, leading to SI and SD scattering cross sections with nucleons at levels of 10^{-45} and 10^{-39} cm 2 , respectively [23]. This theoretical expectation has motivated comprehensive detection efforts through direct [24–28], indirect [29–31], and collider-based approaches [32, 33]. Notably, state-of-the-art direct detection experiments such as LUX-ZEPLIN (LZ) have established unprecedented upper limits on both SI and SD DM-nucleon interactions, constraining these cross sections to below the order of 10^{-47} and 10^{-42} cm 2 respectively [27, 28], while detecting no conclusive signals. These null results collectively imply that the interaction between DM and nucleons is at most feeble.

nature and/or in the processes relevant for its relic density and detection. In the NMSSM, both the bino-dominated and singlino-dominated neutralinos emerge as potential dark matter candidates. Singlino-dominated DM has garnered significant research since the inception of the NMSSM framework [43–62]. The phenomenological behavior of singlino-dominated dark matter is primarily determined by four key parameters: λ , $\tan\beta$, $m_{\tilde{\chi}_1^0}$, and μ_{eff} [43]. In the regime where singlet Higgs bosons are sufficiently massive, both SI and SD DM-nucleon scattering cross sections exhibit a scaling behavior proportional to λ^4 . Consequently, the LZ experiment typically imposes an upper limit of $\lambda \lesssim 0.1$, which implies two primary mechanisms for achieving the observed relic density [44]: (1) co-annihilation with higgsino-dominated EWinos, or (2) resonant annihilations mediated by singlet-dominated CP-even or CP-odd Higgs bosons. To achieve the measured density, the former scenario is only viable within a narrow parameter space characterized by $2|\kappa|/\lambda \simeq 1$, $\lambda < 0.1$, and $\mu < 400$ GeV [43], and the latter scenario requires $2|m_{\tilde{\chi}_1^0}|$ to be close to the scalar mass. Collectively, DM constraints delineate a highly restricted viable parameter space for NMSSM scenarios.

In comparison, dedicated and comprehensive studies on bino-dominated DM in the NMSSM are relatively scarce. This is presumably since the NMSSM does not suggest any direct tree-level coupling between the bino and the new singlet states, rendering the relevant setup largely analogous to MSSM configurations consisting of the bino, higgsinos, and wino [57]. However, in the presence of possibly a light singlet-like scalar state which necessarily accompanies a relatively light singlino-like state [58–65], the NMSSM-specific effects in the EWinos sector become particularly interesting when the soft singlino mass $m_{\tilde{S}} \equiv \frac{2\kappa}{\lambda}\mu_{\text{eff}}$ becomes comparable to both M_1 and μ_{eff} . The singlino-higgsino mixing is directly controlled by the coupling ‘ λ ’, while its mixing with the bino is absent. At the lowest order, such mixing occurs only through the higgsino portal, though it can be enhanced for $|M_1| \lesssim |m_{\tilde{S}}| \sim |\mu_{\text{eff}}|$. Furthermore, the hierarchy between $|m_{\tilde{S}}|$ and $|\mu_{\text{eff}}|$ determines whether the NLSP is predominantly singlino-like ($|m_{\tilde{S}}| < |\mu_{\text{eff}}|$) or higgsino-like ($|m_{\tilde{S}}| > |\mu_{\text{eff}}|$). In the latter scenario, the neutralino sector reduces to a typical bino-higgsino system of the MSSM when the singlino also gets decoupled.

The viability of a highly bino-like DM with a mass below 200 GeV (and particularly below 100 GeV) in the \mathbb{Z}_3 -NMSSM has been extensively studied in Ref. [65]. Such a scenario is highly disfavoured in the MSSM due to current experimental constraints from both collider and cosmological observations. However, this remains viable in the NMSSM without conflicting with bounds from direct detection experiments for DM SI and SD interactions, owing to the emergence of new ‘blind-spots’ as discussed in Ref. [65]. In this context, maintaining a delicate balance between the bino-like LSP and higgsino admixtures is crucial. This balance can be achieved by optimally increasing μ_{eff} , optimally, without requiring it to be just that large when the DM annihilation rate starts suffering, thus leaving too large a relic. The potential for detecting signals of relatively light EWinos and a singlet-like scalar in the context of the \mathbb{Z}_3 -NMSSM, particularly in top squark decays at the LHC, has been discussed in Ref. [66]. Such a spectrum of EWinos and light scalar(s) shown in Refs. [65, 66] bear a further theoretical motivation as this can trigger a strong first-order electroweak phase transition (SFOEWPT) in the early Universe. This could not

only set the stage for a successful electroweak baryogenesis (EWBG) that might explain the experimentally measured baryon asymmetry in the present day Universe, but also could be a potential source of detectable gravitational waves (GWs). Furthermore, phenomenological studies on efficient search-strategies for such light scalars (irrespective of the nature of the LSP) have remained an active area of research [67–86], while Actual searches for these particles constitute a dedicated and vibrant program at the LHC. [87–122]².

In this work, we study in detail status of \mathbb{Z}_3 -NMSSM with a bino-dominated DM (with bino content $> 50\%$) and a light singlet-like scalar vis-a-vis the theoretical and the current experimental constraints (especially the latest LZ experimental limits). In order to obtain an additional light scalar, a choice is made over the Higgs spectrum where the next-to-lightest Higgs is the SM-like Higgs, then the lightest CP -even (-odd) scalar, h_s (a_s), is a singlet-like state. The remainder of this paper is organized as follows. In Section 2, we provide a concise overview of the basic properties of the Z_3 -invariant NMSSM, focusing on the Higgs and neutralino sectors. We then present analytical formulas to demonstrate the DM annihilation and DM-nucleon scattering cross sections. Section 3 outlines our scanning strategy and elucidates the characteristics and status of the model’s parameter space in light of particle physics experiments. Finally, Section 4 summarizes the key findings of this research.

2 Next-to-minimal supersymmetric standard model

2.1 Fundamental NMSSM properties

As the simplest extension of the MSSM, the NMSSM includes one additional gauge singlet Higgs field \hat{S} . The associated superpotential can be expressed as follows [8–10]:

$$W_{\text{NMSSM}} = W_{\text{MSSM}} + \lambda \hat{S} \hat{H}_u \hat{H}_d + \frac{1}{3} \kappa \hat{S}^3, \quad (2.1)$$

where W_{MSSM} is the MSSM superpotential without the μ term, λ and κ are dimensionless parameters, and \hat{H}_u and \hat{H}_d are the common Higgs superfields. It is the most general R-parity-conservation superpotential satisfying a Z_3 discrete symmetry given the considered field content.

Assuming CP-conservation, the Higgs sector of the Z_3 -NMSSM is determined by six parameters at the tree-level [8, 10]:

$$\lambda, \kappa, A_\lambda, A_\kappa, \mu_{eff}, \tan \beta, \quad (2.2)$$

²The non-observation of signals from additional Higgs bosons at the LHC furthermore implies that additional Higgs bosons must either have masses heavier than $2m_t \sim 350\text{GeV}$, or, be dominantly composed of the additional singlet interaction states h_s or a_s such that their production cross section is suppressed. In the NMSSM, the presence of additional light singlet scalars, pseudoscalars, and fermions allows for exotic Higgs decays. According to the latest experimental results from both ATLAS and CMS, non-SM decay modes of the SM-like Higgs boson are not completely ruled out. These experiments have set upper limits on the branching ratio (BR) of such non-SM decays: 12% for ATLAS [3] and 16% for CMS [4]. The LHC experiments are expected to soon constrain the BRs of these non-SM decays beyond the 5-10% level using indirect measurements [123, 124]. It is therefore crucial to leverage LHC Higgs measurements to test BSM models predicting such exotic SM-like Higgs decays.

where A_λ and A_κ are the soft trilinear coefficients defined in Eq. (2.5) of Ref. [8]. In the base-vectors, $H_{\text{SM}} \equiv \sin \beta \text{Re}[H_u^0] + \cos \beta \text{Re}[H_d^0]$, $H_{\text{NSM}} \equiv \cos \beta \text{Re}[H_u^0] - \sin \beta \text{Re}[H_d^0]$, and $H_S \equiv \text{Re}[S]$ for CP-even fields and $A_{\text{NSM}} \equiv \cos \beta \text{Im}[H_u^0] + \sin \beta \text{Im}[H_d^0]$ and $A_S \equiv \text{Im}[S]$ for CP-odd fields³, the three CP-even mass eigenstates $h_i = \{h, H, h_s\}$ and two CP-odd Higgs mass eigenstates $a_i = \{A_H, a_s\}$ are given as follows:

$$\begin{aligned} h_i &= V_{h_i}^{\text{SM}} H_{\text{SM}} + V_{h_i}^{\text{NSM}} H_{\text{NSM}} + V_{h_i}^S H_S, \\ a_i &= V_{a_i}^{\text{NSM}} A_{\text{NSM}} + V_{a_i}^S A_S, \end{aligned} \quad (2.3)$$

where V and V' represent the unitary matrices to diagonalize the corresponding Higgs squared mass matrix. In this work, we denote the physical Higgs state with the largest H_{SM} component by the symbol h , which is called the SM-like Higgs boson hereafter, and we denote the physical Higgs state with the largest non-SM doublet (singlet) component H_{NSM} (H_S) by H (h_s). We also denote the CP-even Higgs bosons by h_1 , h_2 , and h_3 , with $m_{h_1} < m_{h_2} < m_{h_3}$. The latter notation is primarily for convenience. To date, the LHC experiments have measured the couplings of the discovered Higgs boson with about 10% uncertainty, and they revealed that the boson has roughly the same couplings as the SM Higgs boson [125, 126]. These facts imply that $\sqrt{(V_h^{\text{NSM}})^2 + (V_h^S)^2} \lesssim 0.1$ and $|V_h^{\text{SM}}| \sim 1$. Moreover, in the case of very massive charged Higgs bosons, the following approximations hold [23]:

$$V_H^{\text{SM}} \approx V_{h_s}^{\text{SM}} \sim 0, V_H^{\text{NSM}} \approx V_{h_s}^S \approx \left[1 + \left(\frac{V_{h_s}^{\text{NSM}}}{V_{h_s}^S} \right)^2 \right]^{-1/2} \sim 1. \quad (2.4)$$

The singlet masses are independent and may all take small values since they are weakly constrained by current experiments.

In the Z_3 -NMSSM, mixtures of bino (\tilde{B}^0), wino (\tilde{W}^0), higgsino ($\tilde{H}_{d,u}^0$), and singlino (\tilde{S}^0) fields form neutralinos. Assuming a basis of $\psi^0 = (-i\tilde{B}, -i\tilde{W}^0, \tilde{H}_d^0, \tilde{H}_u^0, \tilde{S})$ produces the following neutralino mass matrix [8]:

$$\mathcal{M} = \begin{pmatrix} M_1 & 0 & -m_Z c_\beta s_W & m_Z s_\beta s_W & 0 \\ M_2 & m_Z c_\beta c_W & -m_Z s_\beta c_W & 0 & \\ 0 & -\mu_{\text{eff}} & -\lambda v s_\beta & & \\ 0 & -\lambda v c_\beta & & & \\ \frac{2\kappa}{\lambda} \mu_{\text{eff}} & & & & \end{pmatrix}, \quad (2.5)$$

where M_1 , M_2 , μ_{eff} and $m_{\tilde{S}} \equiv \frac{2\kappa}{\lambda} \mu_{\text{eff}}$ are the soft SUSY-breaking mass parameters of the bino, wino, higgsinos and singlino, respectively; m_Z is the Z -boson mass; θ_w is the Weinberg angle ($c_W \equiv \cos \theta_W$ and $s_W \equiv \sin \theta_W$); $\tan \beta \equiv s_\beta / c_\beta = v_u / v_d$ is the ratio of the vacuum expectation values for the two Higgs doublets ($c_\beta \equiv \cos \beta$ and $s_\beta \equiv \sin \beta$) and $v^2 = v_u^2 + v_d^2 = (174 \text{ GeV})^2$. Diagonalizing M_{neut} with a 5×5 unitary matrix N yields the masses of the physical states $\tilde{\chi}_i^0$ (ordered by mass) of five neutralinos:

$$N^* M_{\text{neut}} N^{-1} = \text{diag}\{m_{\tilde{\chi}_1^0}, m_{\tilde{\chi}_2^0}, m_{\tilde{\chi}_3^0}, m_{\tilde{\chi}_4^0}, m_{\tilde{\chi}_5^0}\}$$

³ H_u^0 , and H_d^0 denote the neutral component fields of the doublet scalar fields H_u and H_d , respectively.

with

$$\tilde{\chi}_i^0 = N_{i1}\tilde{B}^0 + N_{i2}\tilde{W}^0 + N_{i3}\tilde{H}_d^0 + N_{i4}\tilde{H}_u^0 + N_{i5}\tilde{S} \quad (i = 1, 2, 3, 4, 5),$$

where $m_{\tilde{\chi}_i^0}$ is the root to the following characteristic equation:

$$(x - M_1)(x - M_2) [(x^2 - \mu_{eff}^2)(m_{\tilde{S}} - x) + \lambda^2 v^2(x - s_{2\beta}\mu_{eff})] \\ - m_Z^2(x - M_1 c_W^2 - M_2 s_W^2) [(\mu s_{2\beta} + x)(m_{\tilde{S}} - x) + \lambda^2 v^2] = 0. \quad (2.6)$$

The eigenvector of $m_{\tilde{\chi}_i^0}$ is the column vector constituted by $N_{ij}(j = 1, 2, 3, 4, 5)$, which is given by

$$N_i = \frac{1}{\sqrt{C_i}} \begin{pmatrix} (M_2 - m_{\tilde{\chi}_i^0}) [(m_{\tilde{S}} - m_{\tilde{\chi}_i^0}) + \lambda^2 v^2(m_{\tilde{\chi}_i^0} - s_{2\beta}\mu_{eff})] s_W \\ -(M_1 - m_{\tilde{\chi}_i^0}) [(m_{\tilde{S}} - m_{\tilde{\chi}_i^0}) + \lambda^2 v^2(m_{\tilde{\chi}_i^0} - s_{2\beta}\mu_{eff})] c_W \\ -(M_2 s_W^2 + M_1 c_W^2 - m_{\tilde{\chi}_i^0}) [(m_{\tilde{S}} - m_{\tilde{\chi}_i^0})(m_{\tilde{\chi}_i^0} c_\beta + \mu s_\beta) + \lambda^2 v^2 c_\beta] m_Z \\ (M_2 s_W^2 + M_1 c_W^2 - m_{\tilde{\chi}_i^0}) [(m_{\tilde{S}} - m_{\tilde{\chi}_i^0})(m_{\tilde{\chi}_i^0} s_\beta + \mu c_\beta) + \lambda^2 v^2 s_\beta] m_Z \\ (M_2 s_W^2 + M_1 c_W^2 - m_{\tilde{\chi}_i^0}) \lambda v \mu_{eff} c_{2\beta} m_Z \end{pmatrix}. \quad (2.7)$$

The specific form of the normalization factor C_i is:

$$C_i = \left[(m_{\tilde{S}} - m_{\tilde{\chi}_i^0})(m_{\tilde{\chi}_i^0}^2 - \mu_{eff}^2) - \lambda^2 v^2(s_{2\beta}\mu_{eff} - m_{\tilde{\chi}_i^0}) \right]^2 \bullet \\ \left[(M_2 - m_{\tilde{\chi}_i^0})^2 s_W^2 + (M_1 - m_{\tilde{\chi}_i^0})^2 c_W^2 \right] + m_Z^2 (M_2 s_W^2 + M_1 c_W^2 - m_{\tilde{\chi}_i^0})^2 \bullet \\ \left[(m_{\tilde{S}} - m_{\tilde{\chi}_i^0})^2 (\mu_{eff}^2 + m_{\tilde{\chi}_i^0}^2 + 4\mu_{eff} m_{\tilde{\chi}_i^0} s_\beta c_\beta) \right. \\ \left. + 2\lambda^2 v^2 (m_{\tilde{S}} - m_{\tilde{\chi}_i^0})(\mu_{eff} s_{2\beta} + m_{\tilde{\chi}_i^0}) + \lambda^2 v^2 \mu_{eff}^2 c_{2\beta}^2 + \lambda^4 v^4 \right]. \quad (2.8)$$

Then, the diagonalizing matrix is $N = \{N_1, N_2, N_3, N_4, N_5\}$, where $i = 1, 2, 3, 4, 5$ denotes the i -th neutralino.

This work focuses on the lightest neutralino, $\tilde{\chi}_1^0$, which acts as the DM candidate. $N_{11}^2, N_{12}^2, N_{13}^2 + N_{14}^2$, and N_{15}^2 are the bino, wino, higgsino, and singlino components in the physical state $\tilde{\chi}_1^0$, respectively, and satisfy $N_{11}^2 + N_{12}^2 + N_{13}^2 + N_{14}^2 + N_{15}^2 = 1$. If $N_{11}^2 > 0.5$ ($N_{12}^2 > 0.5$, or $N_{13}^2 + N_{14}^2 > 0.5$, or $N_{15}^2 > 0.5$), we call $\tilde{\chi}_1^0$ the bino- (wino-, or higgsino-, or singlino-) dominant DM. In the following discussion, we focus on a bino-dominant $\tilde{\chi}_1^0$ (i.e., $m_{\tilde{\chi}_1^0} \approx M_1$).

The couplings of DM to the scalar Higgs states and Z-boson are included in the calculation of the DM-nucleon cross sections and DM annihilation, which correspond to the Lagrangian [8]:

$$\mathcal{L}_{\text{NMSSM}} \ni iC_{\tilde{\chi}_1^0 \tilde{\chi}_1^0 G^0} G^0 \overline{\tilde{\chi}_1^0} \gamma_5 \tilde{\chi}_1^0 + C_{\tilde{\chi}_1^0 \tilde{\chi}_1^0 h_i} h_i \overline{\tilde{\chi}_1^0} \tilde{\chi}_1^0 + iC_{\tilde{\chi}_1^0 \tilde{\chi}_1^0 a_i} a_i \overline{\tilde{\chi}_1^0} \gamma_5 \tilde{\chi}_1^0 + C_{\tilde{\chi}_1^0 \tilde{\chi}_1^0 Z} Z_\mu \overline{\tilde{\chi}_1^0} \gamma^\mu \gamma_5 \tilde{\chi}_1^0,$$

where the coefficients are given by [8, 23]

$$\begin{aligned} C_{\tilde{\chi}_1^0 \tilde{\chi}_1^0 h_i} &= V_{h_i}^{\text{SM}} \left[\sqrt{2} \lambda N_{15} (N_{13}s_\beta + N_{14}c_\beta) + (g_1 N_{11} - g_2 N_{12}) (N_{13}c_\beta - N_{14}s_\beta) \right] \\ &+ V_{h_i}^{\text{NSM}} \left[\sqrt{2} \lambda N_{15} (N_{13}c_\beta - N_{14}s_\beta) - (g_1 N_{11} - g_2 N_{12}) (N_{13}s_\beta + N_{14}c_\beta) \right] \\ &+ V_{h_i}^{\text{S}} \left[\sqrt{2} (\lambda N_{13}N_{14} - \kappa N_{15}N_{15}) \right], \end{aligned} \quad (2.9)$$

$$\begin{aligned} C_{\tilde{\chi}_1^0 \tilde{\chi}_1^0 a_i} &= -P_{a_i}^{\text{NSM}} \left[\sqrt{2} \lambda N_{15} (N_{13}c_\beta + N_{14}s_\beta) - (g_1 N_{11} - g_2 N_{12}) (N_{13}s_\beta - N_{14}c_\beta) \right] \\ &+ P_{a_i}^{\text{S}} \left[\sqrt{2} (\lambda N_{13}N_{14} - \kappa N_{15}N_{15}) \right], \end{aligned} \quad (2.10)$$

$$C_{\tilde{\chi}_1^0 \tilde{\chi}_1^0 Z} = \frac{m_Z}{\sqrt{2}v} (N_{13}^2 - N_{14}^2), \quad (2.11)$$

$$C_{\tilde{\chi}_1^0 \tilde{\chi}_1^0 G^0} = -\sqrt{2} \lambda N_{15} (N_{13}s_\beta - N_{14}c_\beta) - (g_1 N_{11} - g_2 N_{12}) (N_{13}c_\beta + N_{14}s_\beta). \quad (2.12)$$

It is thus clear that the interactions that are instrumental for the DM phenomenology depend crucially on the higgsino and the singlino admixtures of the LSP which is taken to be bino-dominant in our present study. As we will see later, these admixtures also affect phenomenology at the colliders in a nontrivial manner. It is further noted that such admixtures have rather intricate variations over the NMSSM parameter space. It follows from Eq. (2.5) that variations with $\tan\beta$ and λ might be of particular importance. In addition, the signs on various mass parameters appearing in Eq. (2.5) also have crucial bearings on these admixtures.

2.2 Dark matter sector

When the squark mass $m_{\tilde{q}}$ exceeds 2 TeV, the t-channel Z boson exchange diagram is the dominant contribution to SD scattering cross section at tree-level. This contribution can be parameterized approximately as [127, 128]

$$\sigma_{\tilde{\chi}_1^0 - N}^{\text{SD}} \simeq C_N \times \left(\frac{C_{\tilde{\chi}_1^0 \tilde{\chi}_1^0 Z}}{0.01} \right)^2, \quad (2.13)$$

with $N = p(n)$ denoting protons (neutrons) and $C_p \simeq 2.9 \times 10^{-41} \text{ cm}^2$ ($C_n \simeq 2.3 \times 10^{-41} \text{ cm}^2$) [129, 130]. According to Eq.(2.11), $C_{\tilde{\chi}_1^0 \tilde{\chi}_1^0 Z} \propto N_{13}^2 - N_{14}^2$ [65]. This interaction governs both the DM annihilation cross section through the Z-funnel channel and the SD scattering cross section. Notably, a destructive interference effect (commonly termed a "blind-spot") emerges when $N_{13}^2 \approx N_{14}^2$. Through explicit substitution of N_{13} and N_{14} defined in Eq. (2.7), one can determine

$$\begin{aligned} N_{13}^2 - N_{14}^2 &\approx \frac{m_Z^2 c_{2\beta}}{C_1} (M_2 - m_{\tilde{\chi}_1^0})^2 s_w^4 \bullet \mu_{eff}^4 \bullet \\ &\left[\left(\frac{2\kappa}{\lambda} - \frac{m_{\tilde{\chi}_1^0}}{\mu_{eff}} \right)^2 \left(\frac{m_{\tilde{\chi}_1^0}^2}{\mu_{eff}^2} - 1 \right) + 2 \left(\frac{\lambda v}{\mu_{eff}} \right)^2 \frac{m_{\tilde{\chi}_1^0}}{\mu_{eff}} \left(\frac{2\kappa}{\lambda} - \frac{m_{\tilde{\chi}_1^0}}{\mu_{eff}} \right) + \left(\frac{\lambda v}{\mu_{eff}} \right)^4 \right]. \end{aligned} \quad (2.14)$$

An MSSM-like SD blind-spot condition naturally arises when $\tan \beta = 1$, where $\cos 2\beta$ vanishes [131]. Additionally, significant suppression of the SD cross section becomes feasible when cancellations occur among the bracketed terms in Eq. (2.14), a configuration particularly achievable for a bino-dominated LSP coexisting with light singlino-like states [131]. The algebraic structure reveals three crucial features for a bino-dominated $\tilde{\chi}_1^0$: (i) The first (last) term maintains negative (positive) definiteness; (ii) The second term's sign correlates with the relative sign between $m_{\tilde{S}}$ and $m_{\tilde{\chi}_1^0}$, being positive (negative) for identical (opposite) signs. For coinciding signs, the first term must counterbalance the combined contributions of the latter two terms. Conversely, when signs oppose, cancellation requires mutual annihilation between the aggregated first two terms and the final term – a configuration exhibiting less theoretical naturalness. Crucially, neither $m_{\tilde{S}}$ nor μ_{eff} can significantly exceed the mass of the bino-like LSP in order to maintain an overall cancellation in the presence of the first term.

Another much relevant quantity in the current context is $N_{13}^2 + N_{14}^2$ which is a measure of the total higgsino admixture in the LSP and which controls scalar (Higgs boson) couplings to a pair of bino-like LSPs. Again, using Eq. (2.7), one finds

$$N_{13}^2 + N_{14}^2 = \frac{m_Z^2}{C_1} \left(M_2 s_W^2 + M_1 c_W^2 - m_{\tilde{\chi}_1^0} \right)^2 \bullet \\ \left[(m_{\tilde{S}} - m_{\tilde{\chi}_1^0})^2 (m_{\tilde{\chi}_1^0}^2 + \mu_{eff}^2 + m_{\tilde{\chi}_1^0} \mu_{eff} s_{2\beta}) \right. \\ \left. + 2\lambda^2 v^2 (m_{\tilde{\chi}_1^0} + \mu_{eff} s_{2\beta}) (m_{\tilde{S}} - m_{\tilde{\chi}_1^0}) + \lambda^4 v^4 \right]. \quad (2.15)$$

A little scrutiny reveals that Eqs. (2.14) and (2.15) are all symmetric under simultaneous flips in signs on each of μ_{eff} , $m_{\tilde{\chi}_1^0}$ (M_1) and $m_{\tilde{S}}$.

In contrast, the SI scattering cross section in the heavy squark limit is dominated by a t -channel exchange of CP-even Higgs bosons h_i and is given by [132–135]

$$\sigma_{\tilde{\chi}_1^0 - N}^{SI} = \frac{m_N^2}{2\pi v^2} \left(\frac{m_N m_{\tilde{\chi}_1^0}}{m_N + m_{\tilde{\chi}_1^0}} \right)^2 \left(\frac{1}{125 \text{ GeV}} \right)^4 |f^{(N)}|^2, \\ f^{(N)} = \sum_{i=1}^3 \left(\frac{125 \text{ GeV}}{m_{h_i}} \right)^2 C_{\tilde{\chi}_1^0 \tilde{\chi}_1^0 h_i} C_{h_i NN}. \quad (2.16)$$

$C_{h_i NN}$ is given by [129]

$$C_{h_i NN} = (V_{h_i}^{\text{SM}} - V_{h_i}^{\text{NSM}} \tan \beta) F_d^{(N)} + (V_{h_i}^{\text{SM}} + V_{h_i}^{\text{NSM}} \frac{1}{\tan \beta}) F_u^{(N)}. \quad (2.17)$$

We define

$$\mathcal{B}_d = \sum_{i=1}^3 \left(\frac{125 \text{ GeV}}{m_{h_i}} \right)^2 C_{\tilde{\chi}_1^0 \tilde{\chi}_1^0 h_i} (V_{h_i}^{\text{SM}} - V_{h_i}^{\text{NSM}} \tan \beta), \quad (2.18)$$

$$\mathcal{B}_u = \sum_{i=1}^3 \left(\frac{125 \text{ GeV}}{m_{h_i}} \right)^2 C_{\tilde{\chi}_1^0 \tilde{\chi}_1^0 h_i} (V_{h_i}^{\text{SM}} + V_{h_i}^{\text{NSM}} \frac{1}{\tan \beta}), \quad (2.19)$$

then, $f^{(N)}$ in Eq.(2.16) can be rewritten

$$f^{(N)} = \mathcal{B}_d F_d^{(N)} + \mathcal{B}_u F_u^{(N)}, \quad (2.20)$$

where m_N denotes the nucleon mass, $F_d^{(N)} = f_d^{(N)} + f_s^{(N)} + \frac{2}{27} f_G^{(N)}$ and $F_u^{(N)} = f_u^{(N)} + \frac{4}{27} f_G^{(N)}$ with $f_q^{(N)} = m_N^{-1} \langle N | m_q q\bar{q} | N \rangle$ ($q = u, d, s$) represent the normalized light quark contribution to the nucleon mass, and $f_G^{(N)} = 1 - \sum_{q=u,d,s} f_q^{(N)}$ influences other heavy quark mass fractions in nucleons [134, 135]. For the respective form factors for u, d, s , we adopt the default parameters implemented in micrOMEGAs 5.2 [133]

$$f_{q=u,d,s}^p = \{0.0153, 0.0191, 0.0447\}; \quad f_{q=u,d,s}^n = \{0.011, 0.0273, 0.0447\}, \quad (2.21)$$

resulting in $F_u^{(p)} \simeq 0.152, F_u^{(n)} \simeq 0.147$ and $F_d^{(p)} \simeq 0.132, F_d^{(n)} \simeq 0.140$. Hence, the SI cross sections for DM-proton scattering and DM-neutron scattering are usually approximately equal (i.e., $\sigma_{\tilde{\chi}_1^0-p}^{SI} \simeq \sigma_{\tilde{\chi}_1^0-n}^{SI}$) [136]. However, when \mathcal{B}_d and \mathcal{B}_u in Eq.(2.20) have opposite signs and comparable magnitudes(i.e., a strong cancellation effect), the SI cross sections for protons and neutrons diverge significantly. In such scenarios, the effective cross-section for coherent scattering of DM with xenon nuclei can be computed via [137]

$$\sigma_{\text{eff}}^{\text{SI}} = 0.169\sigma_p^{\text{SI}} + 0.347\sigma_n^{\text{SI}} + 0.484\sqrt{\sigma_p^{\text{SI}}\sigma_n^{\text{SI}}}, \quad (2.22)$$

where the three coefficients on the right side are derived from the average abundances of different xenon isotopes in nature. This equivalence explicitly demonstrates that the effective cross-section reduces to σ_p^{SI} when $\sigma_p^{\text{SI}} = \sigma_n^{\text{SI}}$.

Current LHC experimental constraints require the non-SM doublet Higgs boson H to possess masses exceeding several hundred GeV. Under these conditions, its contribution to the SI cross-section becomes exponentially suppressed through $(125 \text{ GeV}/m_H)^4$. Consequently, the dominant SI scattering mechanisms arise from t-channel exchanges of both the SM-like Higgs h and the singlet Higgs h_s . The h_s -mediated process becomes particularly non-negligible when a significant mass hierarchy exists ($m_{h_s} \ll m_h$), a scenario central to this investigation. For sufficiently large m_H values, our analysis concentrates on these two contributions, leading to the analytical reformulation of Eqs. (2.18) and (2.19):

$$\mathcal{B}_d \approx \left(\frac{125 \text{ GeV}}{m_h}\right)^2 C_{\tilde{\chi}_1^0 \tilde{\chi}_1^0 h} V_h^{\text{SM}} - \left(\frac{125 \text{ GeV}}{m_{h_s}}\right)^2 C_{\tilde{\chi}_1^0 \tilde{\chi}_1^0 h_s} V_{h_s}^{\text{NSM}} \tan \beta, \quad (2.23)$$

$$\mathcal{B}_u \approx \left(\frac{125 \text{ GeV}}{m_h}\right)^2 C_{\tilde{\chi}_1^0 \tilde{\chi}_1^0 h} V_h^{\text{SM}}, \quad (2.24)$$

where we implement the approximations of V_h^{SM} , V_h^{NSM} , $V_{h_s}^{\text{SM}}$ and $V_{h_s}^{\text{NSM}}$ in the Higgs sector above, and the effect of large enough $\tan \beta$ [129]. Under these approximations, for a decoupled wino, by dropping the wino-related term proportional to $g_2 N_{12}$, the generic CP -even scalar-neutralino-neutralino couplings of Eq. (2.9) reduce to

Under this theoretical prescription, when enforcing the wino decoupling condition via elimination of the wino-related term proportional to $g_2 N_{12}$, the generic CP -even scalar-

neutralino-neutralino couplings in Eq. (2.9) reduce to

$$C_{\tilde{\chi}_1^0 \tilde{\chi}_1^0 h} \sim \left[\sqrt{2} \lambda N_{15} (N_{13}s_\beta + N_{14}c_\beta) + g_1 N_{11} (N_{13}c_\beta - N_{14}s_\beta) \right], \quad (2.25)$$

$$C_{\tilde{\chi}_1^0 \tilde{\chi}_1^0 h_s} \sim \left[\sqrt{2} (\lambda N_{13}N_{14} - \kappa N_{15}N_{15}) \right]. \quad (2.26)$$

Substituting N_{11} , N_{13} , N_{14} and N_{15} of Eq. (2.7) into Eqs. (2.25) and (2.26), one finds

$$\begin{aligned} C_{\tilde{\chi}_1^0 \tilde{\chi}_1^0 h} &\sim -\frac{\sqrt{2}m_Z^2 s_W^4 (M_2 - m_{\tilde{\chi}_1^0})^2}{vC_1} \bullet \\ &\left[(m_{\tilde{S}} - m_{\tilde{\chi}_1^0})^2 (m_{\tilde{\chi}_1^0}^2 - \mu_{eff}^2) (m_{\tilde{\chi}_1^0} + \mu_{eff}s_{2\beta}) \right. \\ &+ 2\lambda^2 v^2 (m_{\tilde{S}} - m_{\tilde{\chi}_1^0}) (m_{\tilde{\chi}_1^0}^2 - \mu_{eff}^2) + \lambda^4 v^4 (m_{\tilde{\chi}_1^0} - \mu_{eff}s_{2\beta}) \left. \right]. \end{aligned} \quad (2.27)$$

$$\begin{aligned} C_{\tilde{\chi}_1^0 \tilde{\chi}_1^0 h_s} &\sim \frac{\sqrt{2}m_Z^2 s_W^4 (M_2 - m_{\tilde{\chi}_1^0})^2}{vC_1} \bullet \\ &\left[\lambda v (m_{\tilde{S}} - m_{\tilde{\chi}_1^0})^2 \left[(m_{\tilde{\chi}_1^0}^2 + \mu_{eff}^2)s_\beta c_\beta + m_{\tilde{\chi}_1^0}\mu_{eff} \right] + \kappa\lambda^2 v^3 \mu_{eff}^2 c_{2\beta}^2 \right. \\ &+ \lambda^3 v^3 (m_{\tilde{S}} - m_{\tilde{\chi}_1^0}) (m_{\tilde{\chi}_1^0} s_{2\beta} + \mu_{eff}) + \lambda^5 v^5 s_\beta c_\beta \left. \right] \end{aligned} \quad (2.28)$$

Substituting Eqs. (2.23), (2.24), (2.27) and (2.28) into eq. (2.20), one finds

$$\begin{aligned} f^{(N)} &\approx -\frac{F^N \sqrt{2}m_Z^2 s_W^4 (M_2 - m_{\tilde{\chi}_1^0})^2}{vC_1} \bullet \mu_{eff}^5 \bullet \\ &\left\{ \left(\frac{125GeV}{m_h} \right)^2 2V_h^{\text{SM}} \left[\left(\frac{2\kappa}{\lambda} - \frac{m_{\tilde{\chi}_1^0}}{\mu_{eff}} \right)^2 \left(\frac{m_{\tilde{\chi}_1^0}^2}{\mu_{eff}^2} - 1 \right) \left(\frac{m_{\tilde{\chi}_1^0}}{\mu_{eff}} + s_{2\beta} \right) \right. \right. \\ &+ 2 \left(\frac{\lambda v}{\mu_{eff}} \right)^2 \left(\frac{2\kappa}{\lambda} - \frac{m_{\tilde{\chi}_1^0}}{\mu_{eff}} \right) \left(\frac{m_{\tilde{\chi}_1^0}^2}{\mu_{eff}^2} - 1 \right) + \left(\frac{\lambda v}{\mu_{eff}} \right)^4 \left(\frac{m_{\tilde{\chi}_1^0}}{\mu_{eff}} - s_{2\beta} \right) \left. \right] \\ &+ \left(\frac{125GeV}{m_{h_s}} \right)^2 V_{h_s}^{\text{NSM}} \tan \beta \left[\frac{\lambda v}{\mu_{eff}} \left(\frac{2\kappa}{\lambda} - \frac{m_{\tilde{\chi}_1^0}}{\mu_{eff}} \right)^2 \left[\left(\frac{m_{\tilde{\chi}_1^0}^2}{\mu_{eff}^2} + 1 \right) s_\beta c_\beta + \frac{m_{\tilde{\chi}_1^0}}{\mu_{eff}} \right] \right. \\ &+ \left. \left. \left(\frac{\lambda v}{\mu_{eff}} \right)^2 \kappa v c_{2\beta}^2 + \left(\frac{\lambda v}{\mu_{eff}} \right)^3 \left(\frac{2\kappa}{\lambda} - \frac{m_{\tilde{\chi}_1^0}}{\mu_{eff}} \right) \left(\frac{m_{\tilde{\chi}_1^0}}{\mu_{eff}} s_{2\beta} + 1 \right) + \left(\frac{\lambda v}{\mu_{eff}} \right)^5 s_\beta c_\beta \right] \right\} \end{aligned} \quad (2.29)$$

where we have adopted the assumption $F_d^{(N)} \approx F_u^{(N)} \approx F^{(N)}$. Given $m_{\tilde{\chi}_1^0} \neq M_2, \mu_{eff}, m_{\tilde{S}}$ and $C_1 \neq 0$ for a bino-dominated LSP, blind-spot for the SI cross section arises when the quantity within the big square bracket on the right-hand side of Eq. (2.29) vanishes. This relationship indicates that between h - and h_s -mediated contributions can experience significant cancellation. Such cancellation mechanisms become operative exclusively when

a significant mass hierarchy exists between m_{h_s} and m_h (i.e., $m_{h_s} \ll m_h$). Conversely, in scenarios without this hierarchy, the dominant contribution to $f^{(N)}$ is solely mediated by the SM-like Higgs boson h , leading to a simplified expression:

$$f^{(N)} \approx -\frac{F^N 2\sqrt{2}m_Z^2 s_W^4 (M_2 - m_{\tilde{\chi}_1^0})^2}{v C_1} \bullet \mu_{eff}^5 \bullet \\ \left(\frac{125 GeV}{m_h} \right)^2 \left[\left(\frac{2\kappa}{\lambda} - \frac{m_{\tilde{\chi}_1^0}}{\mu_{eff}} \right)^2 \left(\frac{m_{\tilde{\chi}_1^0}^2}{\mu_{eff}^2} - 1 \right) \left(\frac{m_{\tilde{\chi}_1^0}}{\mu_{eff}} + s_{2\beta} \right) \right. \\ \left. + 2 \left(\frac{\lambda v}{\mu_{eff}} \right)^2 \left(\frac{2\kappa}{\lambda} - \frac{m_{\tilde{\chi}_1^0}}{\mu_{eff}} \right) \left(\frac{m_{\tilde{\chi}_1^0}^2}{\mu_{eff}^2} - 1 \right) + \left(\frac{\lambda v}{\mu_{eff}} \right)^4 \left(\frac{m_{\tilde{\chi}_1^0}}{\mu_{eff}} - s_{2\beta} \right) \right], \quad (2.30)$$

where a vanishing $C_{\tilde{\chi}_1^0 \tilde{\chi}_1^0 h}$ results in a blind-spot of the SI scattering cross section.

The observed DM relic density is $\Omega_{DM} h^2 \simeq 0.12$ [34], where $h \equiv H_0/(100 \text{ km/s/Mpc})$ parameterizes the Hubble constant and $\Omega_{DM} \equiv \rho_{DM}/\rho_c$ is the DM density in units of the critical density. As a viable DM candidate, the relic density of $\tilde{\chi}_1^0$, which we denote as $\Omega_{\tilde{\chi}_1^0} \equiv \rho_{\tilde{\chi}_1^0}/\rho_c$, should match the observed value Ω_{DM} . For DM produced via standard thermal freeze-out (FO), the relic density and the effective (thermally averaged) annihilation cross section at freeze out, $\langle \sigma v \rangle_{FO}$, are approximately related as

$$\Omega_{\tilde{\chi}_1^0} h^2 \sim 0.1 \times \frac{3 \times 10^{-26} \text{ cm}^3/\text{s}}{\langle \sigma v \rangle_{FO}}. \quad (2.31)$$

Since at the time of freeze-out (parameterized by the temperature $x \equiv m_{\tilde{\chi}_1^0}/T$) the DM candidate is usually non-relativistic (typically, $x^{FO} \sim 20$), one often expands $\langle \sigma v \rangle_{FO}$ as

$$\langle \sigma v \rangle_{x_F} = a + 6b/x_F + \mathcal{O}(x_F^{-2}). \quad (2.32)$$

In the presence of comparably light singlet-like states, the Bino-dominated DM candidate can be by the funnels (scalars), or the co-annihilation with a Singlino-dominated neutralino to achieve the measured abundance [65]. If the LSP has a non-negligible higgsino component, it can efficiently annihilate into a pair of gauge bosons and doublet-like Higgs bosons via s -channel Z or Higgs exchange, as well as through t -channel neutralino and chargino exchange. For sufficiently heavy LSPs ($m_{\tilde{\chi}_1^0} > m_t$), annihilation into a pair of top quarks via Higgs exchange can significantly contribute. In the large $\tan \beta$ regime, where the Higgs couplings to $b\bar{b}$ and $\tau^+\tau^-$ are enhanced, $b\bar{b}$ and $\tau^+\tau^-$ final states are possible via s -channel Higgs exchange (not necessarily resonant). Moreover, in the case where the additional scalar/pseudoscalars are light, new final states can be kinematically allowed: for example, annihilation into $Z h_s$, $h_s h_s$, $h_s a_s$ and $a_s a_s$ can significantly contribute to the reduction of the neutralino relic density, either via s -channel Z , h_s , a_s , or t -channel (heavier) neutralino exchange. Here the NMSSM specific couplings λ and κ can play an important role.

3 Numerical Results

3.1 Research strategy

We first used the `NMSSMTools-6.0.0` package [138, 139] to perform a sophisticated scan over the following parameter space:

$$\begin{aligned} 0.0 < \lambda \leq 0.75, \quad |\kappa| \leq 0.75, \quad 1 \leq \tan \beta \leq 60, \\ 0.1 \text{ TeV} < |\mu| \leq 1.5 \text{ TeV}, \quad |A_\lambda| \leq 5 \text{ TeV}, \quad |A_\kappa| \leq 1.5 \text{ TeV}, \\ |M_1| \leq 1.5 \text{ TeV}, \quad 0.1 \text{ TeV} \leq M_2 \leq 1.5 \text{ TeV}, \\ |A_t| = |A_b| \leq 5 \text{ TeV}, \quad 0.1 \text{ TeV} \leq M_{\tilde{l}_L}, M_{\tilde{l}_R} \leq 1.5 \text{ TeV}, \end{aligned}$$

in which all parameters were defined at the scale $Q = 1$ TeV. To obtain the SM-like Higgs boson mass ($m_h \approx 125$ GeV), the soft trilinear coefficients A_t and A_b were assumed to be equal and freely change to adjust the Higgs mass spectrum. The masses of the left (right) three generation sleptons take a common value $M_{\tilde{l}_L}(M_{\tilde{l}_R})$, which was used as free parameters to explain the muon g-2 anomaly, to relax the LHC restrictions. Other unimportant parameters were fixed at 3 TeV, including the gluino mass M_3 , the masses of three generations squarks, and all soft trilinear coefficients except A_t and A_b . We also required $N_{11}^2 > 0.5$ in the scan to achieve a bino-dominated $\tilde{\chi}_1^0$.

Specifically, we carried out the MultiNest algorithm [140, 141] with $n_{\text{live}} = 5000$ ⁴ to scan comprehensively the parameter space. The following likelihood function was constructed to guide the scan to get the samples satisfying these experiments:

$$\mathcal{L} = \mathcal{L}_{m_h} \times \mathcal{L}_{h,\text{coupling}} \times \mathcal{L}_B \times \mathcal{L}_{\Omega h^2} \times \mathcal{L}_{DM} \times \mathcal{L}_{\Delta a_\mu}, \quad (3.1)$$

where

- \mathcal{L}_{m_h} and $\mathcal{L}_{h,\text{coupling}}$ are likelihood functions for the experimentally measured SM-like Higgs boson mass and couplings, respectively. The computation of m_h included leading electroweak corrections, two loop terms, and propagator corrections, as in Ref. [142]. Its experimental central value was taken as $m_h = 125.09$ GeV [21], and a total experimental and theoretical uncertainty of 3 GeV was assumed. $\mathcal{L}_{h,\text{coupling}}$ works in a seven-parameter κ -framework with related experimental measurements, such as the central values and uncertainties of the Higgs couplings and their correlation coefficients, taken from the ATLAS analysis, using 80fb^{-1} data collected during the LHC Run-II [125]. Some knowledge about probability and statistics was used in constructing $\mathcal{L}_{h,\text{coupling}}$ (see the introduction in Ref. [143]).
- \mathcal{L}_B is the likelihood function for the measured branching ratio of the $B \rightarrow X_s \gamma$ and $B_s \rightarrow \mu^+ \mu^-$. These ratios were calculated by the formulae in Refs. [144, 145] and should be consistent with their experimental measurements at the 2σ level [143].

⁴The n_{live} parameter in the algorithm controls the number of active points sampled in each iteration of the scan.

- $\mathcal{L}_{\Omega h^2}$ and \mathcal{L}_{DM} are likelihood functions for the measured abundance from the WMAP/Planck experiments [34] and the detection of both SI and SD DM-nucleon scattering cross-sections, respectively. For \mathcal{L}_{DM} , we modeled it with a Gaussian distribution centered at zero and defined $\delta_\sigma^2 = \text{UL}_\sigma^2 / 1.64^2 + (0.2\sigma)^2$, where UL_σ refers to the upper limit of the LZ(2022) results [27] on the DM-nucleon SI and SD scattering rate at a 90% C. L., and 0.2σ accounts for theoretical uncertainties [146]. For DM relic density, we take the central value of $\Omega h^2 = 0.120$ from the Planck-2018 data [34] and assume theoretical uncertainties of 20%, i.e., $0.096 \leq \Omega h^2 \leq 0.144$. Relevant quantities were calculated using the `micrOMEGAs` package [147–150].
- $\mathcal{L}_{\Delta a_\mu}$ is the likelihood function of the muon $g - 2$ anomaly given by

$$\mathcal{L}_{\Delta a_\mu} = \exp \left[-\frac{\chi_{\Delta a_\mu}^2}{2} \right] = \exp \left[-\frac{1}{2} \left(\frac{a_\mu^{\text{SUSY}} - 2.49 \times 10^{-9}}{4.8 \times 10^{-10}} \right)^2 \right] \quad (3.2)$$

where $\Delta a_\mu \equiv a_\mu^{\text{Exp}} - a_\mu^{\text{SM}}$ is the difference between experimental central value of a_μ and its SM prediction. Taking into account the latest measurement by the Fermilab Muon $g - 2$ Experiment [151], the combined experimental average a_μ^{Exp} shows a 5.1σ discrepancy with the community-approved SM prediction a_μ^{SM} from the Muon $g - 2$ Theory Initiative [152],

$$\Delta a_\mu = a_\mu^{\text{Exp}} - a_\mu^{\text{SM}} = (2.49 \pm 0.48) \times 10^{-9}. \quad (3.3)$$

which implies the presence of potential new physics (NP) effects. While it is essential to acknowledge that uncertainties in the computation of leading-order hadronic contributions may contribute to the observed deviation [153, 154]⁵, there has been considerable interest in exploring the BSM origin of this anomaly [162, 163].

The acquired samples were further refined using the following criteria: the SM-like Higgs mass was within the range of 122–128 GeV, and a p-value tested by the code `HiggsSignals-2.6.2` [164–167] was larger than 0.05 which guarantees the SM-like Higgs' properties to be consistent with corresponding measurements by the ATLAS and CMS collaborations at the 95% confidence level, and extra Higgs searches were implemented through the code `HiggsBounds-5.10.2` [168–172], and $\kappa^2 + \lambda^2 < 0.5$ so that the theory keeps perturbative up to 10^{16} GeV scale [173], and the observed DM relic abundance was within $\pm 10\%$ of the measured central value $\Omega h^2 = 0.12$ (i.e., $0.108 \leq \Omega h^2 \leq 0.132$) [34].

⁵The potential underestimation of theoretical uncertainties has been a subject of debate, thereby impeding the establishment of a conclusive comparison of the muon $g - 2$ measurement with theoretical predictions at present [155–157]. Notably, the Budapest-Marseille-Wuppertal (BMW) collaboration conducted lattice calculations on the leading-order hadronic vacuum polarization contribution, achieving sub-percent precision as detailed in [158]. This effort mitigated the observed discrepancy to a margin of 1.5σ [159]. Additionally, the determination of dispersive relations, utilizing the latest $e^+e^- \rightarrow \pi^+\pi^-$ cross section measurements by the CMD-3 experiment, demonstrates good alignment with the combined FermiLab-BNL result, despite exhibiting a discrepancy with all previous results [160, 161].

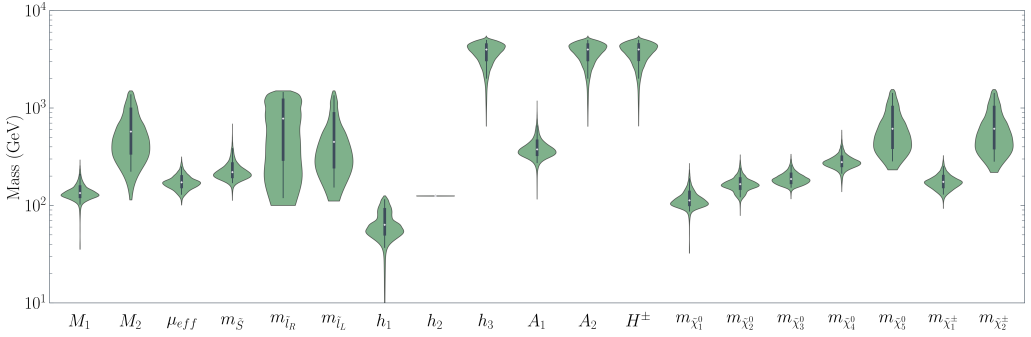


Figure 1. Violin plots showing mass distributions of Higgs, EWinos and sleptons for the refined samples. The violins are scaled by count. Thick vertical bar in center indicates interquartile range with white dot representing the median; long vertical line represents 95% confidence interval.

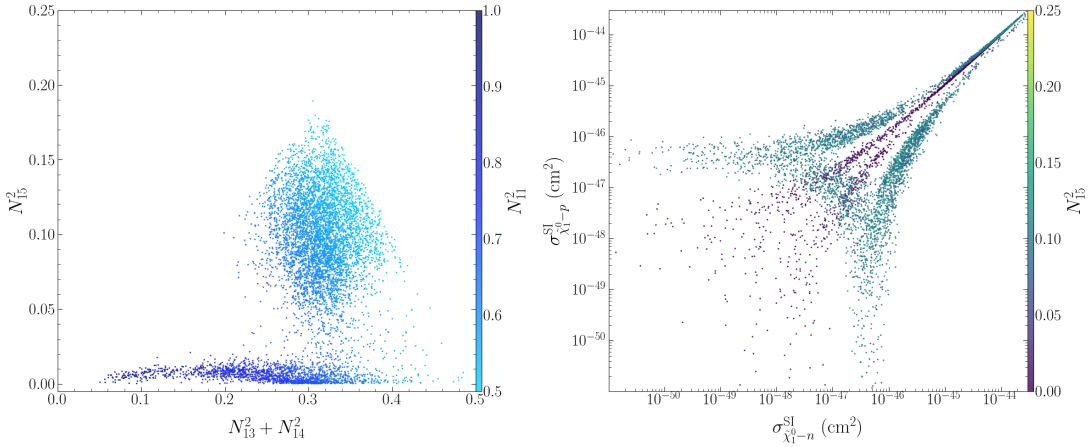


Figure 2. The left panel displayed the components of $\tilde{\chi}_1^0$ for the refined samples. In the right panel, the refined samples were projected onto the $\sigma_{\tilde{\chi}_1^0 - p}^{SI}$ – $\sigma_{\tilde{\chi}_1^0 - n}^{SI}$ plane, with colors representing the values of N_{15}^2 .

Firstly, for the refined samples, the mass distributions of the Higgs and SUSY particles were shown in Fig. 1 using violin plots⁶. From Fig. 1, one can find that h_2 is the SM-like Higgs (h) and $m_{h_1} \leq m_{h_2} \ll m_{h_3}$, i.e., in the presence of a light singlet-like scalar state ($h_s \equiv h_1$). In this case, as the discussion on DM-nucleon cross section as in Section 2.2, the contribution from non-SM doublet Higgs bosons ($H \equiv h_3$) to the SI cross section is suppressed by $(125/m_H)^4$. Moreover, the contribution to SI scattering cross section of h_s -mediated process may become particularly non-negligible due to existing a significant mass hierarchy between m_{h_s} and m_h . For masses of EWinos, $M_1 \in (-291, -35)$ GeV \cup $(36, 293)$ GeV, $\mu_{eff} \in (-311, -101)$ GeV \cup $(102, 305)$ GeV, $m_{\tilde{S}} \in (-687, -125)$ GeV \cup $(112, 564)$ GeV, $M_2 \in (114, 1500)$ GeV, $|\mu_{eff}/M_1| \in (1.2, 4.53)$, $|m_{\tilde{S}}/\mu_{eff}| \in (1.0, 3.9)$, $|m_{\tilde{\chi}_1^0}/M_1| \in (0.71, 0.98)$, $|m_{\tilde{\chi}_2^0}/\mu_{eff}| \in (0.7, 1.13)$, $|m_{\tilde{\chi}_3^0}/\mu_{eff}| \in (1.0, 1.33)$, $|m_{\tilde{\chi}_4^0}/m_{\tilde{S}}| \in (0.7, 1.5)$ and $|m_{\tilde{\chi}_1^\pm}/\mu_{eff}| \in (0.7, 1.0)$. Thus, the setup features one light chargino and four relatively light neutralinos with the lightest one of them (the LSP)

⁶A violin plot combines the advantages of the box plot and probability density distribution plot [174].

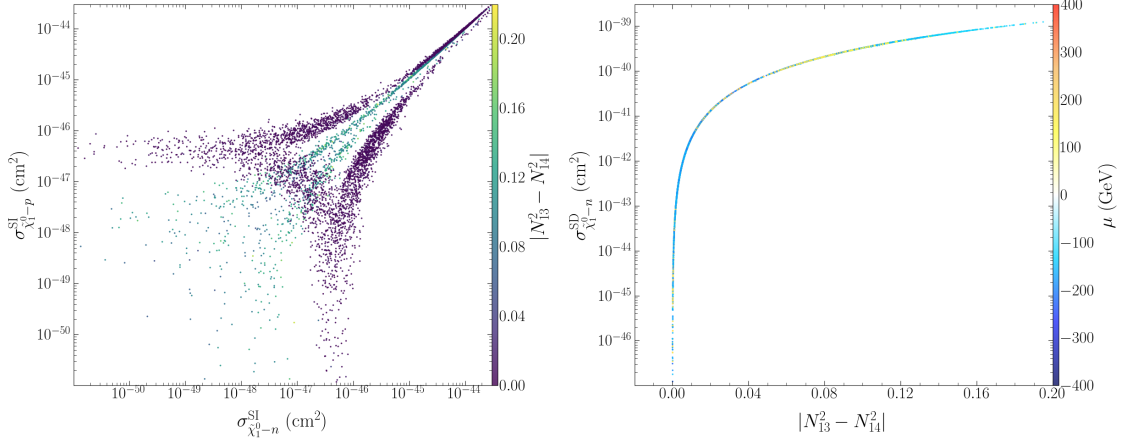


Figure 3. Projection of the refined samples onto the $\sigma_{\tilde{\chi}_1^0-p}^{SI}$ – $\sigma_{\tilde{\chi}_1^0-n}^{SI}$ plane, where colors indicated $|N_{13}^2 - N_{14}^2|$ values (left panel), and onto the $\sigma_{\tilde{\chi}_1^0-n}^{SD}$ – $|N_{13}^2 - N_{14}^2|$ plane with colors representing μ_{eff} values (right panel).

being bino-dominant. The composition of $\tilde{\chi}_1^0$ was illustrated on the left panel of Fig. 2. It can be observed that the inventory points can be categorized into two systems based on the composition of $\tilde{\chi}_1^0$: a bino-higgsino system ($N_{15}^2 < 0.05$) and a bino-higgsino-singlino system ($N_{15}^2 > 0.05$). From the right panel of Fig. 2 and Fig. 3, it is evident that the DM-nucleon cross sections of the two dark matter systems display significant differences. Next, we will investigate the specific challenges related to direct detection, indirect detection and relic density of dark matter for the refined samples.

3.2 Dark Matter phenomenology

As illustrated in Fig. 3, the bino-higgsino system is significantly constrained by LZ experiment on SD cross section. This can be attributed to the fact that σ^{SD} is proportional to $|N_{13}^2 - N_{14}^2|$, and these samples exhibit large values of $|N_{13}^2 - N_{14}^2|$. Additionally, We check components of other neutralinos and find that $\tilde{\chi}_{2,3}^0$ and $\tilde{\chi}_1^\pm$ are higgsino-dominant, and $\tilde{\chi}_4^0$ is singlino-dominant, where DM phenomenology at the LHC would mostly resemble an MSSM scenario with a higgsino-like NLSP [74]. In this context, σ^{SD} is suppressed by $1/\mu_{eff}^4$, and the LZ experiment requires $\mu_{eff} > 380$ GeV [35]. In contrast, for the bino-higgsino-singlino system, the values of $|N_{13}^2 - N_{14}^2|$ approach zero corresponding to blind-spot condition as given in Eq.(2.14), which results in $\sigma_{\tilde{\chi}_1^0-n}^{SD}$ as low as 10^{-50} cm². A moderate to large value of ‘λ’ ($0.3 < \lambda < 0.7$) is found to play a deciding role in an adequate tempering of a bino LSP with higgsino (and hence singlino) admixture. We analyzed the case carefully and find that $1 < m_{\tilde{S}}/m_{\tilde{\chi}_1^0} < 3$ (i.e., $m_{\tilde{S}}$ and $m_{\tilde{\chi}_1^0}$ have the same signs where the cancellation in Eq.(2.14) occurs between the first term and the sum of the rest two, and $m_{\tilde{S}}$ is not much larger than the mass $m_{\tilde{\chi}_1^0}$). However, this induces a critically large bino-singlino mixing in the $\tilde{\chi}_1^0$ which in turn could be disfavored by the constraints on the SI rates (see the results presented by $\sigma_{\tilde{\chi}_1^0-p}^{SI}$ – $\sigma_{\tilde{\chi}_1^0-n}^{SI}$ panel in Figures 2 and 3). In any case, this is again purely an NMSSM phenomenon showcasing a tempering of the bino-dominated LSP by the singlino which necessarily has to be assisted by the higgsinos.

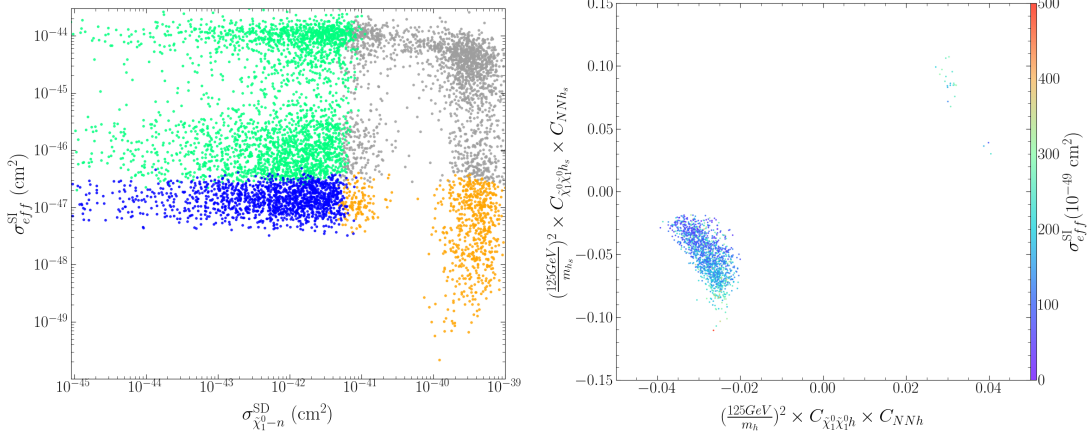


Figure 4. In the left panel, the refined samples were projected onto the σ_{eff}^{SI} – $\sigma_{\tilde{\chi}_1^0 - n}^{SD}$ plane. Here, grey samples were excluded by both the LZ(2022) limits on the SI and SD cross sections for dark matter-neutron scattering. In contrast, orange and green samples were excluded by either one of these limits, while blue samples remained viable under all constraints. In the right panel, the surviving blue dots from the left panel were projected onto the $(\frac{125 \text{ GeV}}{m_{h_s}})^2 \times C_{\tilde{\chi}_1^0 \tilde{\chi}_1^0 h_s} \times C_{NNh_s}$ – $(\frac{125 \text{ GeV}}{m_h})^2 \times C_{\tilde{\chi}_1^0 \tilde{\chi}_1^0 h} \times C_{NNh}$ plane, where the color bar indicated the values of σ_{eff}^{SI} .

It should be pointed out that after considering the limitations of LZ(2022) experiments in both SI and SD cross sections, the SI cross sections for proton and neutron at survival points show that when one value is significantly higher, its counterpart may be relatively lower. Thus, σ_{eff}^{SI} in Eq.(2.22) is calculated, and the refined samples are plotted onto the σ_{eff}^{SI} – $\sigma_{\tilde{\chi}_1^0 - n}^{SD}$ panel of Fig. 3. Grey samples are excluded by both the LZ(2022) limits on the SI and SD cross sections for dark matter-neutron scattering. Conversely, orange and green samples are excluded by either one of these limits, while blue samples remain viable under all constraints which has been ruled out by recent WIMP search results from LZ(2024) [28] which seem to rule out thermally-produced natural SUSY WIMPs. For these surviving samples, the contribution to SI scattering coming from the t-channel exchange of SM-like Higgs bosons h and the singlet Higgs boson h_s are projected onto the right panel of Fig. 3 with the color bar indicating the values of σ_{eff}^{SI} . One can see that the t-channel exchange of the singlet Higgs boson h_s is the main contribution, with large $|(\frac{125 \text{ GeV}}{m_{h_s}})^2 \times C_{\tilde{\chi}_1^0 \tilde{\chi}_1^0 h_s} \times C_{NNh_s}|$ values resulting in large σ_{eff}^{SI} . Table 1 shows parameter ranges for the samples satisfied the LZ limits on the SI and SD cross sections for dark matter-neutron scattering. Because h_s is much lighter than h , the primary contribution to SI scattering may come from the t-channel exchange of the singlet Higgs boson h_s .

Any DM candidate is also subject to constraints from indirect detection experiments. Here we briefly discussed on direct detection constraints on these surviving samples. Given the substantial astrophysical uncertainties associated with charged particle production in indirect detection, we focused on constraints from photon emission. For these surviving samples, as illustrated in Fig. 6, we analyzed contributions to $\langle \sigma v \rangle_{x_F}$, demonstrating that the dominant contribution originates from the annihilation channel $\tilde{\chi}_1^0 \tilde{\chi}_1^0 \rightarrow W^+ W^-$ which

Table 1. Parameter ranges for the samples satisfied the LZ(2022) limits on both the SI and SD cross sections for dark matter-neutron scattering. Quantities with mass dimension are in unit of GeV.

para	range	para	range	para	range
$\tan \beta$	$9 \sim 34$	A_t	$-2650 \sim 2250$	$m_{\tilde{\chi}_1^0}$	$(-212 \sim -70) \cup (93 \sim 160)$
κ	$(-0.39 \sim -0.18) \cup (0.16 \sim 0.43)$	m_{h_1}	$33 \sim 75$	$m_{\tilde{\chi}_2^0}$	$(-270 \sim -130) \cup (118 \sim 221)$
λ	$0.31 \sim 0.63$	m_{h_2}	$125 \sim 126$	$m_{\tilde{\chi}_3^0}$	$(-255 \sim -146) \cup (144 \sim 298)$
μ	$(-283 \sim -128) \cup (144 \sim 254)$	m_{h_3}	$1640 \sim 5190$	$m_{\tilde{\chi}_4^0}$	$(-387 \sim -201) \cup (219 \sim 329)$
M_1	$(-236 \sim -91) \cup (115 \sim 184)$	m_{A_1}	$251 \sim 569$	$m_{\tilde{\chi}_5^0}$	$(-337 \sim -238) \cup (245 \sim 1535)$
M_2	$142 \sim 1490$	m_{A_2}	$1640 \sim 5190$	$m_{\tilde{\chi}_1^\pm}$	$113 \sim 291$
A_λ	$(-5000 \sim -1500) \cup (2070 \sim 5000)$	m_{H^\pm}	$1640 \sim 5209$	$m_{\tilde{\chi}_2^\pm}$	$(-1493 \sim -220) \cup (244 \sim 1535)$
A_κ	$(-593 \sim -418) \cup (271 \sim 810)$	$m_{\tilde{l}_L}$	$119 \sim 1490$	$m_{\tilde{l}_R}$	$100 \sim 1500$

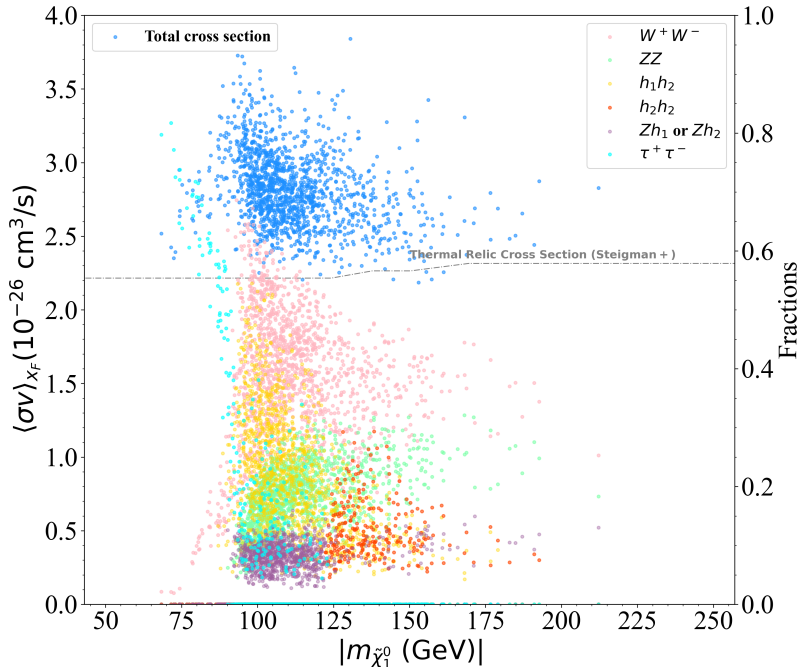


Figure 5. The surviving samples coupling with the LZ2022 limits were projected onto the $\langle\sigma v\rangle_{x_F} - m_{\tilde{\chi}_1^0}$ plane. The blue dots represent the total cross section, while the pink, green, orange, red, purple, and cyan dots correspond to the fractions of the annihilation channels $\tilde{\chi}_1^0 \tilde{\chi}_1^0 \rightarrow W^+W^-$, ZZ , $h_1 h_2$, $h_2 h_2$, $Z h_1$ or $Z h_2$, $\tau^+\tau^-$, respectively.

exhibits significant interference with other channels including $\tilde{\chi}_1^0 \tilde{\chi}_1^0 \rightarrow ZZ$, $h_1 h_2$, $h_2 h_2$, $Z h_1$, and $Z h_2$. These processes occur in the mass range $95\text{GeV} \lesssim m_{\tilde{\chi}_1^0} \lesssim 200\text{GeV}$. Additionally, the major contribution of a few individual points from $\tilde{\chi}_1^0 \tilde{\chi}_1^0 \rightarrow \tau^+\tau^-$ with $70\text{GeV} \lesssim m_{\tilde{\chi}_1^0} \lesssim 95\text{GeV}$. Current stringent indirect detection constraints on WIMP DM come from Fermi-LAT and MAGIC analyses of Milky Way satellite galaxies, rul-

Final state	Production mode	m_s range [GeV]	\mathcal{L} [fb^{-1}]	Collaboration
$\mu\mu\mu\mu$	gg fusion	[4, 8] \cup [11.5, 60]	137	CMS [110]
		[1.2, 2] \cup [4.4, 8] \cup [12, 60]	139	ATLAS [108]
$\mu\mu\tau\tau$	gg fusion	[15, 62.5]	35.9	CMS [98]
$bb\mu\mu$	gg fusion	[18, 60]	139	ATLAS [111]
		[20, 62.5]	35.9	CMS [112]
$bb\tau\tau$	gg fusion	[15, 60]	35.9	CMS [103]
$bbbb$	Wh/Zh	[20, 60]	36.1	ATLAS [120]
$\gamma\gamma\gamma\gamma$	gg fusion	[15, 60]	132	CMS [121]
$\gamma\gamma jj$	VBF	[20, 60]	36.7	ATLAS [109]

Table 2. The existing experimental searches for exotic Higgs decays $h \rightarrow ss \rightarrow XXYY$ at the 13 TeV LHC. Modified from Table 1 of Ref. [83].

ing out canonical values of the thermally averaged annihilation cross sections $\langle\sigma v\rangle \sim 2 \times 10^{-26} \text{ cm}^3 \text{ s}^{-1}$ for DM masses $m_\chi \lesssim 100 \text{ GeV}$ when annihilations dominantly produce b -quark or τ -lepton pairs [175–177]. For DM masses $m_{\tilde{\chi}_1^0} \gtrsim 100 \text{ GeV}$, indirect detection bounds weaken significantly. Relevant constraints might further arise from the annihilation of DM matter particles captured via elastic scattering in the Sun, potentially giving rise to a flux of neutrinos observable at Earth. Under certain assumptions [178], most relevant for our case if DM annihilates dominantly into pairs of W bosons, current bounds from DM capture and annihilation yield the most constraining upper limits on the spin dependent DM-proton scattering cross section [178–180], where neutrinos from capture in the Sun give the strongest bound on the SD scattering cross section excluding $\sigma_p^{SD} \gtrsim 10^{-40} \text{ cm}^2$ for $m_{\tilde{\chi}_1^0} \lesssim 1 \text{ TeV}$. In our model’s parameter space, which satisfies relic density requirements and direct detection constraints (SIDD/SDDD), the annihilation channel $\tilde{\chi}_1^0 \tilde{\chi}_1^0 \rightarrow W^+ W^-$ exhibits interference with competing channels, resulting in relatively weak solar neutrino constraints.

3.3 Collider constraints

The results presented in the previous section demonstrate that light neutralino DM sustains a minimal yet viable survival capacity under the LZ(2022) experiment. Building on these results, we examined the collider phenomenology of such candidates through the following analysis.

Firstly, we examine the constraints imposed by the invisible decay of the SM-like Higgs boson. According to Table 1, the mass range for the lightest Higgs boson (h_1) is (30, 75) GeV. For $30 \text{ GeV} < m_{h_1} < m_h/2 \approx 63 \text{ GeV}$, the decay channel $h_2 \rightarrow h_1 h_1$ is kinematically allowed. This mass range can be extended up to approximately 75 GeV by including additional three-body decays. As m_{h_1} increases, the decay channel becomes progressively off-shell, thereby diminishing its significance. The decay $h_2 \rightarrow h_1 h_1$ yields various final states determined by the subsequent decay channels of the lighter scalar h_1 .

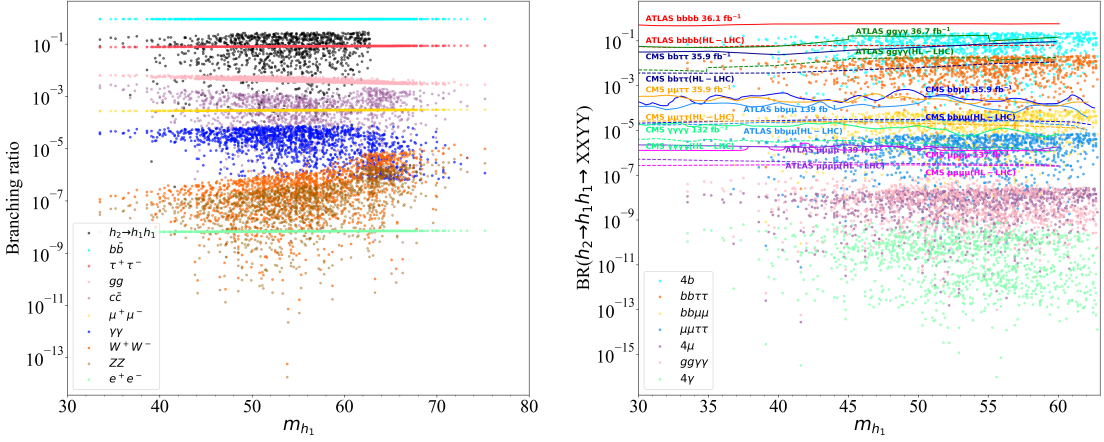


Figure 6. Left panel: Branching ratios of exotic decays of the SM-like Higgs boson (h_2) and Branching ratios of CP-even singlet Higgs (h_1) to SM particles. Right panel: Branching ratio of $h_2 \rightarrow h_1 h_1 \rightarrow XXYY$ for the surviving samples coupling with the LZ2022 limits, current bounds (solid lines) and corresponding projections at the the high-luminosity LHC (HL-LHC) (dash lines).

These final states can be generically represented as $XXYY$, where X and Y denote distinct SM particles. Typically, for $m_{h_1} > 2m_b \sim 10$ GeV, the dominant final state is $h_2 \rightarrow h_1 h_1 \rightarrow bbbb$, whereas for $m_{h_1} < 10$ GeV, the predominant final states are $gggg$, $gg\tau\tau$, and $\tau\tau\tau\tau$ [84–86]. In Table 2, we summarized existing LHC searches for $h \rightarrow ss \rightarrow XXYY$, where the scalar particle s has a mass in the range 30 – 63 GeV. This table lists the targeted final states, production mechanisms, corresponding integrated luminosities, and the intermediate scalar s mass ranges covered in each analysis. Notably, all LHC searches for final states other than $bbbb$ require at least one pair of non-hadronic signatures, such as photons, muons, or τ leptons. The left panel of Fig. 6 displayed the branching ratios for both the exotic decay of the SM-like Higgs boson ($h_2 \rightarrow h_1 h_1$) and the subsequent decays of the CP-even singlet Higgs (h_1) into SM particles. The right panel of Fig. 6 illustrated the branching ratio of the sequential decay $h_2 \rightarrow h_1 h_1 \rightarrow XXYY$ for the surviving parameter points (dots), superimposed with current experimental bounds (solid curves) and projected HL-LHC sensitivity (dashed curves). The HL-LHC projections are derived using the simple assumption that all uncertainties can be taken to scale as $1/\sqrt{L}$ [83]. Regions above the exclusion curves are ruled out by existing searches. All $XXYY$ decay channels for the surviving parameter points remain consistent with current experimental limits. Even under HL-LHC projections, the $b\bar{b}b\bar{b}$, $b\bar{b}\tau\bar{\tau}$, and $b\bar{b}\mu\bar{\mu}$ final states retain significant parameter space while satisfying constraints. Furthermore, the $\mu\bar{\mu}\tau\bar{\tau}$, $\mu\bar{\mu}\mu\bar{\mu}$, $gg\gamma\gamma$, and $\gamma\gamma\gamma\gamma$ final states fully comply with all imposed limits.

Next, we evaluated whether the surviving parameter samples satisfy constraints from LHC EWino searches by program **SModelS-3.0.0** [181], which incorporates the experimental selection efficiencies listed in Table 3. We find that the direct EWino searches in the WZ mediated, $2l + E_T^{\text{miss}}$ channel [193] and the Wh_{125} mediated $1l + 2b + E_T^{\text{miss}}$ channel [197] implemented in **SModelS-3.0.0** play a dominant role. The mass ranges

Table 3. Experimental analyses included in the package **SModels-3.0.0**.

Name	Scenario	Final State	Luminosity(fb ⁻¹)
ATLAS-1402-7029 [182]	$\tilde{\chi}_1^\pm \tilde{\chi}_2^0 \rightarrow \ell \bar{\nu} \ell \ell (\bar{\nu} \nu), \ell \bar{\nu} \ell \ell (\bar{\nu} \nu) \rightarrow \ell \bar{\nu} \tilde{\chi}_1^0 \ell \ell (\nu \nu) \tilde{\chi}_1^0$ $\tilde{\chi}_1^\pm \tilde{\chi}_2^0 \rightarrow W^\pm \tilde{\chi}_1^0 Z \tilde{\chi}_1^0 \rightarrow \ell \bar{\nu} \tilde{\chi}_1^0 \ell \ell \tilde{\chi}_1^0$ $\tilde{\chi}_1^\pm \tilde{\chi}_2^0 \rightarrow W^\pm \tilde{\chi}_1^0 h \tilde{\chi}_1^0 \rightarrow \ell \bar{\nu} \tilde{\chi}_1^0 \ell \ell \tilde{\chi}_1^0$	$3\ell + E_T^{\text{miss}}$	20.3
CMS-SUS-16-034 [183]	$\tilde{\chi}_2^0 \tilde{\chi}_1^\pm \rightarrow W \tilde{\chi}_1^0 Z(h) \tilde{\chi}_1^0$	$n\ell(n>=2) + n j(n>=1) + E_T^{\text{miss}}$	35.9
CMS-SUS-16-039 [184]	$\tilde{\chi}_2^0 \tilde{\chi}_1^\pm \rightarrow \ell \bar{\nu} \ell \ell$ $\tilde{\chi}_2^0 \tilde{\chi}_1^\pm \rightarrow \tilde{\tau} \bar{\nu} \ell \ell$ $\tilde{\chi}_2^0 \tilde{\chi}_1^\pm \rightarrow \tilde{\tau} \nu \tilde{\tau} \tau$ $\tilde{\chi}_2^0 \tilde{\chi}_1^\pm \rightarrow W Z \tilde{\chi}_1^0 \tilde{\chi}_1^0$ $\tilde{\chi}_2^0 \tilde{\chi}_1^\pm \rightarrow W H \tilde{\chi}_1^0 \tilde{\chi}_1^0$	$n\ell(n>0)(\tau) + E_T^{\text{miss}}$	35.9
CMS-SUS-16-045 [185]	$\tilde{\chi}_2^0 \tilde{\chi}_1^\pm \rightarrow W^\pm \tilde{\chi}_1^0 h \tilde{\chi}_1^0$	$1\ell~2b + E_T^{\text{miss}}$	35.9
CMS-SUS-16-048 [186]	$\tilde{\chi}_2^0 \tilde{\chi}_1^\pm \rightarrow Z \tilde{\chi}_1^0 W \tilde{\chi}_1^0$ $\tilde{\chi}_2^0 \tilde{\chi}_1^0 \rightarrow Z \tilde{\chi}_1^0 \tilde{\chi}_1^0$	$2\ell + E_T^{\text{miss}}$	35.9
CMS-SUS-17-004 [187]	$\tilde{\chi}_2^0 \tilde{\chi}_1^\pm \rightarrow Wh(Z) \tilde{\chi}_1^0 \tilde{\chi}_1^0$	$n\ell(n>=0) + n j(n>=0) + E_T^{\text{miss}}$	35.9
CMS-SUS-17-009 [188]	$\tilde{\ell} \bar{\ell} \rightarrow \ell \tilde{\chi}_1^0 \ell \tilde{\chi}_1^0$	$2\ell + E_T^{\text{miss}}$	35.9
CMS-SUS-17-010 [189]	$\tilde{\chi}_1^\pm \tilde{\chi}_1^\mp \rightarrow W^\pm \tilde{\chi}_1^0 W^\mp \tilde{\chi}_1^0$ $\tilde{\chi}_1^\pm \tilde{\chi}_1^\mp \rightarrow \nu \bar{\ell} \ell \bar{\nu}$	$2\ell + E_T^{\text{miss}}$	35.9
ATLAS-1803-02762 [190]	$\tilde{\chi}_2^0 \tilde{\chi}_1^\pm \rightarrow W Z \tilde{\chi}_1^0 \tilde{\chi}_1^0$ $\tilde{\chi}_2^0 \tilde{\chi}_1^\pm \rightarrow \nu \bar{\ell} \ell \bar{\nu}$ $\tilde{\chi}_1^\pm \tilde{\chi}_1^\mp \rightarrow \nu \bar{\ell} \nu \bar{\ell}$ $\tilde{\ell} \bar{\ell} \rightarrow \ell \tilde{\chi}_1^0 \ell \tilde{\chi}_1^0$	$n\ell~(n>=2) + E_T^{\text{miss}}$	36.1
ATLAS-1806-02293 [191]	$\tilde{\chi}_2^0 \tilde{\chi}_1^\pm \rightarrow W Z \tilde{\chi}_1^0 \tilde{\chi}_1^0$	$n\ell(n>=2) + n j(n>=0) + E_T^{\text{miss}}$	36.1
ATLAS-1812-09432 [192]	$\tilde{\chi}_2^0 \tilde{\chi}_1^\pm \rightarrow Wh \tilde{\chi}_1^0 \tilde{\chi}_1^0$	$n\ell~(n>=0) + n j(n>=0) + nb(n>=0) + n \gamma(n>=0) + E_T^{\text{miss}}$	36.1
CMS-SUS-20-001 [193]	$\tilde{\chi}_2^0 \tilde{\chi}_1^\pm \rightarrow Z \tilde{\chi}_1^0 W \tilde{\chi}_1^0$ $\tilde{\ell} \bar{\ell} \rightarrow \ell \tilde{\chi}_1^0 \ell \tilde{\chi}_1^0$	$2\ell + E_T^{\text{miss}}$	137
CMS-SUS-20-004 [194]	$\tilde{\chi}_2^0 \tilde{\chi}_3^0 \rightarrow h \tilde{\chi}_1^0 h \tilde{\chi}_1^0$	$4b + E_T^{\text{miss}}$	137
CMS-SUS-21-002 [195]	$\tilde{\chi}_1^\pm \tilde{\chi}_1^\mp \rightarrow W^\pm \tilde{\chi}_1^0 W^\mp \tilde{\chi}_1^0$ $\tilde{\chi}_{2/3}^0 \tilde{\chi}_1^\pm \rightarrow W^\pm \tilde{\chi}_1^0 Z(h) \tilde{\chi}_1^0$ $\tilde{\chi}_2^0 \tilde{\chi}_3^0 \rightarrow Z \tilde{\chi}_1^0 h \tilde{\chi}_1^0$	$4b + E_T^{\text{miss}}$	137
ATLAS-1908-08215 [196]	$\tilde{\ell} \bar{\ell} \rightarrow \ell \tilde{\chi}_1^0 \ell \tilde{\chi}_1^0$ $\tilde{\chi}_1^\pm \tilde{\chi}_1^\mp$	$2\ell + E_T^{\text{miss}}$	139
ATLAS-1909-09226 [197]	$\tilde{\chi}_2^0 \tilde{\chi}_1^\pm \rightarrow Wh \tilde{\chi}_1^0 \tilde{\chi}_1^0$	$1\ell + h(\rightarrow bb) + E_T^{\text{miss}}$	139
ATLAS-1911-12606 [198]	$\tilde{\chi}_2^0 \tilde{\chi}_1^\pm \rightarrow Z \tilde{\chi}_1^0 W \tilde{\chi}_1^0$ $\tilde{\chi}_2^0 \tilde{\chi}_1^0 \rightarrow Z \tilde{\chi}_1^0 \tilde{\chi}_1^0$ $\tilde{\chi}_1^\pm \tilde{\chi}_1^\mp \rightarrow W^\pm \tilde{\chi}_1^0 W^\mp \tilde{\chi}_1^0$ $\tilde{\ell} \bar{\ell} \rightarrow \ell \tilde{\chi}_1^0 \ell \tilde{\chi}_1^0$	$2\ell + 2j + E_T^{\text{miss}}$	139
ATLAS-1912-08479 [199]	$\tilde{\chi}_2^0 \tilde{\chi}_1^\pm \rightarrow W(\rightarrow l\nu) \tilde{\chi}_1^0 Z(\rightarrow \ell\ell) \tilde{\chi}_1^0$	$3\ell + E_T^{\text{miss}}$	139
ATLAS-2106-01676 [200]	$\tilde{\chi}_1^\pm \tilde{\chi}_2^0 \rightarrow W(\rightarrow l\nu) Z(\rightarrow \ell\ell) \tilde{\chi}_1^0 \tilde{\chi}_1^0$ $\tilde{\chi}_1^\pm \tilde{\chi}_2^0 \rightarrow W(\rightarrow l\nu) h(\rightarrow \ell\ell) \tilde{\chi}_1^0 \tilde{\chi}_1^0$	$3\ell + E_T^{\text{miss}}$	139
ATLAS-2108-07586 [201]	$\tilde{\chi}_1^\pm \tilde{\chi}_1^\mp \rightarrow WW \tilde{\chi}_1^0 \tilde{\chi}_1^0$ $\tilde{\chi}_1^\pm \tilde{\chi}_2^0 \rightarrow WZ(h) \tilde{\chi}_1^0 \tilde{\chi}_1^0$	$4j + E_T^{\text{miss}}$	139
ATLAS-2204-13072 [202]	$\tilde{\chi}_2^0 \tilde{\chi}_1^\pm \rightarrow W(\rightarrow qq) \tilde{\chi}_1^0 Z(\rightarrow \ell\ell) \tilde{\chi}_1^0$	$2\ell + 2j + E_T^{\text{miss}}$	139
ATLAS-2209-13935 [203]	$\tilde{\ell} \bar{\ell} \rightarrow \ell \bar{\ell} \tilde{\chi}_1^0 \tilde{\chi}_1^0$ $\tilde{\chi}_1^\pm \tilde{\chi}_1^\mp \rightarrow W(\rightarrow \ell\nu) W(\rightarrow \ell\nu) \tilde{\chi}_1^0 \tilde{\chi}_1^0$	$2\ell + E_T^{\text{miss}}$	139

$140\text{Gev} < \tilde{\chi}_2^0 \approx \tilde{\chi}_1^\pm < 260\text{Gev}$ and $45\text{Gev} < \Delta m = \tilde{\chi}_2^0 - \tilde{\chi}_1^0 < 65\text{Gev}$ for the samples passed the limitations from the LHC search for the electroweakinos. The kind of spectrum

is tightly constrained at the LHC.

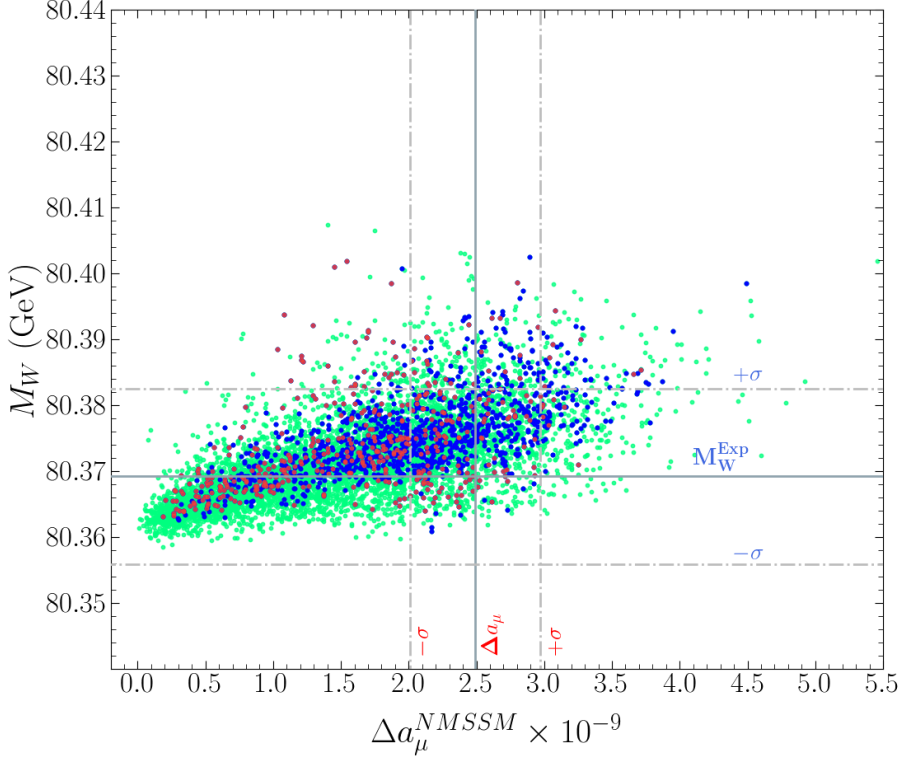


Figure 7. Results for the surviving scenarios in the $\Delta a_\mu - M_W$ plane. Green, blue and red points indicate all the refined samples, the surviving samples coupling with the LZ2022 limits, and the samples which passes the LZ2022 limits and the limits from direct EWino searches in program `SModelS-3.0.0`, respectively. The vertical grey lines indicate the central value of Δa_μ as given in Eq. (3.3) (solid) and its $\pm 1\sigma$ range (dashed). The horizontal grey lines indicate the current central value for the world average without CDF II of the W boson mass M_W^{exp} (solid), and its $\pm 1\sigma$ uncertainties (dashed).

Finally, we projected the results onto the $\Delta a_\mu - M_W$ plane in Fig.7, where green, blue and red points indicate all the refined samples, the surviving samples coupling with the LZ(2022) limits, and the samples which passes the LZ(2022) limits and the limits from direct EWino searches in program `SModelS-3.0.0`, respectively. The vertical grey lines indicate the central value of Δa_μ as given in Eq. (3.3) (solid), and its $\pm 1\sigma$ range (dashed). The horizontal grey lines indicate the current central value for the world average without CDF II of the W boson mass M_W^{exp} (solid), and its $\pm 1\sigma$ uncertainties (dashed) [143, 204]⁷.

⁷A recent combination of W -boson mass measurements performed by the ATLAS, LHCb, CDF, and D0 experiments, using a careful calibration of simulation tools and PDFs, obtained the world average, $M_W = 80.3946 \pm 0.0115 GeV$ [204]. However, the probability of compatibility is 0.5% or less, depending on the chosen PDF set, which is mostly due to the W mass measurement by CDF from Run II at the Tevatron [204], $M_W = 80.432 \pm 0.016 GeV$ (adjusted to the common PDF set CT18 [205] in Ref. [204]). It differs by almost 3.6σ from the other measurements of M_W , while the latter agree well among each other, with the

Interestingly, the particle spectra obtained by scanning can well describe both M_W and a_μ . It is evident that the predicted values of M_W for the majority of the refined samples fall within the 1σ confidence interval of M_W^{Exp} . A minor proportion of samples exhibit predicted values that exceed the upper bound of this confidence interval. This phenomenon can be attributed to the fact that the corresponding regions feature light EWinos in the 100 GeV–1 TeV range, such that the electroweakly-interacting SUSY particles generate sufficiently large contributions to M_W . Moreover, for smaller values of Δa_μ , the lower values of M_W^{NMSSM} are indicative of heavier electroweak supersymmetric particle masses. Thus, the relatively light SUSY particles that are required for larger values of Δa_μ give rise to a slight increase in the prediction for M_W that is independent of the variation of the other parameters in the scan. These conclusions are similar to the studies in Ref. [206–208].

4 Conclusion

Inspired by the rapid progress of particle physics experiments in recent years, we studied their impacts on the \mathbb{Z}_3 -NMSSM with a light bino-dominated LSP and a light singlet-like scalar and how the theory kept consistent with them. We are particularly interested in the recent measurement of the muon g-2 at Fermilab, the LHC search for SUSY, and the DM direct detection by the LZ experiment since they are sensitive to different parameters and complement each other to provide valuable information of the \mathbb{Z}_3 -NMSSM.

Motivated by the substantial advancements in particle physics experiments over recent years, we have investigated the effects of these developments on the \mathbb{Z}_3 -NMSSM featuring a light bino-dominated LSP and a light singlet-like scalar, while evaluating the theory's consistency with experimental constraints. Our focus encompasses the latest muon g-2 results from Fermilab, SUSY particle searches at the LHC, and DM direct detection by the LZ experiment since they are sensitive to different parameters and complement each other to provide valuable information of the \mathbb{Z}_3 -NMSSM.

We initiated our investigation by employing the MultiNest algorithm for a comprehensive parameter space scan, guided by the LZ(2022) experiments, while incorporating constraints from the LHC Higgs data, muon g-2 observable, and B-physics measurements. The surviving samples were categorized into bino-higgsino ($N_{15}^2 < 0.05$) and bino-higgsino-singlino ($N_{15}^2 > 0.05$) systems based on the composition of $\tilde{\chi}_1^0$. These systems exhibit annihilation channels into W^+W^- , ZZ , h_1h_2 , h_2h_2 , Zh_1 , and Zh_2 to satisfy relic density requirements, facilitated by both a non-negligible higgsino component in the LSP and the presence of a light singlet-like scalar. However, their viability is challenged by stringent dark matter direct detection constraints. Although σ^{SI} of the bino-higgsino system under the blind-spot condition can be below the experimental limit of LZ(2022) as well as the neutrino floor, its σ^{SD} is significantly constrained by LZ experiment on SD cross section due large $|N_{13}^2 - N_{14}^2|$ values, which is somewhat similar to MSSM scenario with a higgsino-like NLSP [74] and a larger μ_{eff} under the LZ(2022) experiment is necessary [35, 36]. In contrast, for the bino-higgsino-singlino system, the values of $|N_{13}^2 - N_{14}^2|$ approach zero corresponding to blind-spot condition for the SD scattering cross section, which results in

average without CDF II $M_W = 80.3692 \pm 0.0133\text{GeV}$ [204].

$\sigma_{\tilde{\chi}_1^0 - n}^{SD}$ as low as 10^{-50} cm 2 . However, this induces a critically large bino-singlino mixing in the LSP which in turn could be disfavored by the constraints on the SI rates. A moderate to large value of ‘ λ ’ ($0.3 < \lambda < 0.7$) is found to play a deciding role in an adequate tempering of a bino LSP with higgsino (and hence singlino) admixture. It should be noted that the SI cross section of protons and neutrons in the bino-higgsino-singlino system are abnormal below the order of 10^{-46} cm 2 , that is, when one value is significantly higher, its counterpart may be relatively lower. This may be related to the small difference between $F_{q=u,d}^{(p)}$ and $F_{q=u,d}^{(n)}$. In this case, we use the effective cross section when considering the restriction of DMDD on SI cross section.

Exotic Higgs decays are a cornerstone of the discovery program at both current and future colliders [209–214]. For the surviving samples coupling with the LZ(2022) limits, the mass range for the lightest Higgs boson (h_1) is (30, 75) GeV. For $30 \text{ GeV} < m_{h_1} < m_h/2 \approx 63$ GeV, the decay channel $h_2 \rightarrow h_1 h_1$ is kinematically allowed. So, we examine the constraints imposed by the invisible decay of the SM-like Higgs boson. A dedicated search for exotic Higgs decays can actively explore this framework at the LHC, while future exotic Higgs decay searches at the high-luminosity LHC and future Higgs factories will be vital to conclusively probe the scenario. At the HL-LHC, detector upgrades, new trigger and analysis strategies, and increased datasets will steadily increase the sensitivity to small branching ratios, especially in subdominant but cleaner final states (notably $h \rightarrow ss \rightarrow bb\tau\tau$, $h \rightarrow \text{invisible}$) [215, 216]. Meanwhile, proposed e^+e^- colliders offer lower integrated luminosities but substantially lower backgrounds, resulting in excellent sensitivity to challenging all-hadronic modes, notably $h \rightarrow ss \rightarrow bbbb$ [217]. In addition, the surviving scenario is featured by $M_1 \in (-291, -35)$ GeV \cup (36, 293) GeV, $\mu_{eff} \in (-311, -101)$ GeV \cup (102, 305) GeV, $m_{\tilde{S}} \in (-687, -125)$ GeV \cup (112, 564) GeV, $M_2 \in (114, 1500)$ GeV, $|\mu_{eff}/M_1| \in (1.2, 4.53)$, $|m_{\tilde{S}}/\mu_{eff}| \in (1.0, 3.9)$, $|m_{\tilde{\chi}_1^0}/M_1| \in (0.71, 0.98)$, $|m_{\tilde{\chi}_2^0}/\mu_{eff}| \in (0.7, 1.13)$, $|m_{\tilde{\chi}_3^0}/\mu_{eff}| \in (1.0, 1.33)$, $|m_{\tilde{\chi}_4^0}/m_{\tilde{S}}| \in (0.7, 1.5)$ and $|m_{\tilde{\chi}_1^\pm}/\mu_{eff}| \in (0.7, 1.0)$, which is tightly constrained by the direct searches of EWinos at the LHC in the modes $pp \rightarrow m_{\tilde{\chi}_1^\pm} m_{\tilde{\chi}_2^0} \rightarrow m_{\tilde{\chi}_1^0} W^{\pm(*)}, m_{\tilde{\chi}_1^0} Z^{(*)}/h_{SM}$, but can simultaneously describe M_W and a_μ .

In summary, the \mathbb{Z}_3 -NMSSM featuring a light bino-dominated LSP and a light singlet-like scalar faces significant tension with increasingly stringent upper limits on both SI and SD DM-nucleus elastic scattering cross sections, as well as constraints from LHC EWino searches. Nevertheless, this scenario retains the capacity to naturally accommodate the observed Z boson mass, reproduce the SM-like Higgs boson mass, account for the muon anomalous magnetic moment, and generate substantial contributions to the W boson mass. It can still predict Z boson mass, the SM-like Higgs boson mass in a natural way, and explain Muon Anomalous Magnetic Moment, and also lead to sizable contributions to W boson mass. In any case, these are purely an NMSSM phenomenon showcasing a tempering of the bino-dominated LSP by the singlino which necessarily has to be assisted by the higgsinos.

Acknowledgments

We sincerely thank Prof. Junjie Cao for numerous helpful discussions.

References

- [1] G. Aad *et al.* [ATLAS], Phys. Lett. B **716** (2012), 1-29 doi:10.1016/j.physletb.2012.08.020 [arXiv:1207.7214 [hep-ex]].
- [2] S. Chatrchyan *et al.* [CMS], Phys. Lett. B **716** (2012), 30-61 doi:10.1016/j.physletb.2012.08.021 [arXiv:1207.7235 [hep-ex]].
- [3] G. Aad *et al.* [ATLAS], Nature **607**, no.7917, 52-59 (2022) [erratum: Nature **612**, no.7941, E24 (2022)] doi:10.1038/s41586-022-04893-w [arXiv:2207.00092 [hep-ex]].
- [4] A. Tumasyan *et al.* [CMS], Nature **607**, no.7917, 60-68 (2022) [erratum: Nature **623**, no.7985, E4 (2023)] doi:10.1038/s41586-022-04892-x [arXiv:2207.00043 [hep-ex]].
- [5] H. E. Haber and G. L. Kane, Phys. Rept. **117**, 75 (1985). doi:10.1016/0370-1573(85)90051-1
- [6] J. F. Gunion and H. E. Haber, Nucl. Phys. B **272**, 1 (1986) Erratum: [Nucl. Phys. B **402**, 567 (1993)]. doi:10.1016/0550-3213(86)90340-8, 10.1016/0550-3213(93)90653-7
- [7] H. E. Haber and M. Sher, Phys. Rev. D **35**, 2206 (1987). doi:10.1103/PhysRevD.35.2206
- [8] U. Ellwanger, C. Hugonie and A. M. Teixeira, Phys. Rept. **496**, 1 (2010) doi:10.1016/j.physrep.2010.07.001 [arXiv:0910.1785 [hep-ph]].
- [9] M. Maniatis, Int. J. Mod. Phys. A **25** (2010), 3505-3602 doi:10.1142/S0217751X10049827 [arXiv:0906.0777 [hep-ph]].
- [10] K. Cheung, T. J. Hou, J. S. Lee and E. Senaha, Phys. Rev. D **82**, 075007 (2010) doi:10.1103/PhysRevD.82.075007 [arXiv:1006.1458 [hep-ph]].
- [11] J. E. Kim and H. P. Nilles, *Phys. Lett.* **B138** (1984) 150.
- [12] M. Bastero-Gil, C. Hugonie, S. F. King, D. P. Roy and S. Vempati, Phys. Lett. B **489** (2000), 359-366 doi:10.1016/S0370-2693(00)00930-8 [arXiv:hep-ph/0006198 [hep-ph]].
- [13] L. J. Hall, D. Pinner and J. T. Ruderman, JHEP **1204**, 131 (2012) doi:10.1007/JHEP04(2012)131 [arXiv:1112.2703 [hep-ph]].
- [14] U. Ellwanger, JHEP **03** (2012), 044 doi:10.1007/JHEP03(2012)044 [arXiv:1112.3548 [hep-ph]].
- [15] J. F. Gunion, Y. Jiang and S. Kraml, Phys. Lett. B **710** (2012), 454-459 doi:10.1016/j.physletb.2012.03.027 [arXiv:1201.0982 [hep-ph]].
- [16] S. F. King, M. Mühlleitner and R. Nevzorov, Nucl. Phys. B **860** (2012), 207-244 doi:10.1016/j.nuclphysb.2012.02.010 [arXiv:1201.2671 [hep-ph]].
- [17] D. Albornoz Vasquez, G. Belanger, C. Boehm, J. Da Silva, P. Richardson and C. Wymant, Phys. Rev. D **86** (2012), 035023 doi:10.1103/PhysRevD.86.035023 [arXiv:1203.3446 [hep-ph]].
- [18] J. J. Cao, Z. X. Heng, J. M. Yang, Y. M. Zhang and J. Y. Zhu, JHEP **1203**, 086 (2012) doi:10.1007/JHEP03(2012)086 [arXiv:1202.5821 [hep-ph]].
- [19] S. F. King, M. Mühlleitner, R. Nevzorov and K. Walz, Nucl. Phys. B **870**, 323 (2013) doi:10.1016/j.nuclphysb.2013.01.020 [arXiv:1211.5074 [hep-ph]].
- [20] Z. Kang, J. Li and T. Li, JHEP **11** (2012), 024 doi:10.1007/JHEP11(2012)024 [arXiv:1201.5305 [hep-ph]].

- [21] G. Aad *et al.* [ATLAS and CMS], Phys. Rev. Lett. **114**, 191803 (2015) doi:10.1103/PhysRevLett.114.191803 [arXiv:1503.07589 [hep-ex]].
- [22] G. Jungman, M. Kamionkowski and K. Griest, Phys. Rept. **267**, 195-373 (1996) doi:10.1016/0370-1573(95)00058-5 [arXiv:hep-ph/9506380 [hep-ph]].
- [23] S. Baum, M. Carena, N. R. Shah and C. E. M. Wagner, JHEP **1804**, 069 (2018) doi:10.1007/JHEP04(2018)069 [arXiv:1712.09873 [hep-ph]].
- [24] E. Aprile *et al.* [XENON], Phys. Rev. Lett. **121** (2018) no.11, 111302 doi:10.1103/PhysRevLett.121.111302 [arXiv:1805.12562 [astro-ph.CO]].
- [25] Q. Wang *et al.* [PandaX-II], Chin. Phys. C **44** (2020) no.12, 125001 doi:10.1088/1674-1137/abb658 [arXiv:2007.15469 [astro-ph.CO]].
- [26] X. Cui *et al.* [PandaX-II], Phys. Rev. Lett. **119** (2017) no.18, 181302 doi:10.1103/PhysRevLett.119.181302 [arXiv:1708.06917 [astro-ph.CO]].
- [27] J. Aalbers *et al.* [LZ], Phys. Rev. Lett. **131** (2023) no.4, 041002 doi:10.1103/PhysRevLett.131.041002 [arXiv:2207.03764 [hep-ex]].
- [28] J. Aalbers *et al.* [LZ], [arXiv:2410.17036 [hep-ex]].
- [29] O. Adriani *et al.* [PAMELA], Phys. Rev. Lett. **105** (2010), 121101 doi:10.1103/PhysRevLett.105.121101 [arXiv:1007.0821 [astro-ph.HE]].
- [30] M. Ackermann *et al.* [Fermi-LAT], Phys. Rev. Lett. **108** (2012), 011103 doi:10.1103/PhysRevLett.108.011103 [arXiv:1109.0521 [astro-ph.HE]].
- [31] M. Aguilar *et al.* [AMS 01], Phys. Lett. B **646** (2007), 145-154 doi:10.1016/j.physletb.2007.01.024 [arXiv:astro-ph/0703154 [astro-ph]].
- [32] J. Goodman, M. Ibe, A. Rajaraman, W. Shepherd, T. M. P. Tait and H. B. Yu, Phys. Lett. B **695** (2011), 185-188 doi:10.1016/j.physletb.2010.11.009 [arXiv:1005.1286 [hep-ph]].
- [33] P. J. Fox, R. Harnik, J. Kopp and Y. Tsai, Phys. Rev. D **85** (2012), 056011 doi:10.1103/PhysRevD.85.056011 [arXiv:1109.4398 [hep-ph]].
- [34] N. Aghanim *et al.* [Planck], Astron. Astrophys. **641** (2020), A6 [erratum: Astron. Astrophys. **652** (2021), C4] doi:10.1051/0004-6361/201833910 [arXiv:1807.06209 [astro-ph.CO]].
- [35] Y. He, L. Meng, Y. Yue and D. Zhang, Phys. Rev. D **108**, no.11, 115010 (2023) doi:10.1103/PhysRevD.108.115010 [arXiv:2303.02360 [hep-ph]].
- [36] D. Li, L. Meng and H. Zhou, Nucl. Phys. B **1005**, 116591 (2024) doi:10.1016/j.nuclphysb.2024.116591 [arXiv:2312.01594 [hep-ph]].
- [37] S. Bisal, A. Chatterjee, D. Das and S. A. Pasha, Phys. Rev. D **110** (2024) no.2, 023043 doi:10.1103/PhysRevD.110.023043 [arXiv:2311.09937 [hep-ph]].
- [38] S. Bisal, A. Chatterjee, D. Das and S. A. Pasha, Phys. Rev. D **110** (2024) no.1, 015021 doi:10.1103/PhysRevD.110.015021 [arXiv:2311.09938 [hep-ph]].
- [39] G. F. Giudice and A. Masiero, Phys. Lett. B **206** (1988), 480-484 doi:10.1016/0370-2693(88)91613-9
- [40] A. Arvanitaki, M. Baryakhtar, X. Huang, K. van Tilburg and G. Villadoro, JHEP **03** (2014), 022 doi:10.1007/JHEP03(2014)022 [arXiv:1309.3568 [hep-ph]].

- [41] J. A. Evans, Y. Kats, D. Shih and M. J. Strassler, JHEP **07** (2014), 101 doi:10.1007/JHEP07(2014)101 [arXiv:1310.5758 [hep-ph]].
- [42] H. Baer, V. Barger, D. Mickelson and M. Padelfke-Kirkland, Phys. Rev. D **89** (2014) no.11, 115019 doi:10.1103/PhysRevD.89.115019 [arXiv:1404.2277 [hep-ph]].
- [43] H. Zhou, J. Cao, J. Lian and D. Zhang, Phys. Rev. D **104** (2021) no.1, 015017 doi:10.1103/PhysRevD.104.015017 [arXiv:2102.05309 [hep-ph]].
- [44] J. Cao, Y. He, L. Shang, Y. Zhang and P. Zhu, Phys. Rev. D **99**, no. 7, 075020 (2019) doi:10.1103/PhysRevD.99.075020 [arXiv:1810.09143 [hep-ph]].
- [45] J. Cao, L. Meng, Y. Yue, H. Zhou and P. Zhu, Phys. Rev. D **101**, no. 7, 075003 (2020) doi:10.1103/PhysRevD.101.075003 [arXiv:1910.14317 [hep-ph]].
- [46] D. Das, U. Ellwanger and A. M. Teixeira, JHEP **1204**, 067 (2012) doi:10.1007/JHEP04(2012)067 [arXiv:1202.5244 [hep-ph]].
- [47] Q. F. Xiang, X. J. Bi, P. F. Yin and Z. H. Yu, Phys. Rev. D **94** (2016) no.5, 055031 doi:10.1103/PhysRevD.94.055031 [arXiv:1606.02149 [hep-ph]].
- [48] F. Domingo, J. S. Kim, V. M. Lozano, P. Martin-Ramiro and R. Ruiz de Austri, Phys. Rev. D **101** (2020) no.7, 075010 doi:10.1103/PhysRevD.101.075010 [arXiv:1812.05186 [hep-ph]].
- [49] S. Baum, N. R. Shah and K. Freese, JHEP **04** (2019), 011 doi:10.1007/JHEP04(2019)011 [arXiv:1901.02332 [hep-ph]].
- [50] M. van Beekveld, S. Caron and R. Ruiz de Austri, JHEP **01** (2020), 147 doi:10.1007/JHEP01(2020)147 [arXiv:1906.10706 [hep-ph]].
- [51] A. Chatterjee, A. Datta and S. Roy, JHEP **06** (2022), 108 doi:10.1007/JHEP06(2022)108 [arXiv:2202.12476 [hep-ph]].
- [52] J. Cao, F. Li, J. Lian, Y. Pan and D. Zhang, Sci. China Phys. Mech. Astron. **65** (2022) no.9, 291012 doi:10.1007/s11433-022-1927-9 [arXiv:2204.04710 [hep-ph]].
- [53] J. Cao, L. Meng and Y. Yue, Phys. Rev. D **108** (2023) no.3, 035043 doi:10.1103/PhysRevD.108.035043 [arXiv:2306.06854 [hep-ph]].
- [54] S. Roy and C. E. M. Wagner, JHEP **04** (2024), 106 doi:10.1007/JHEP04(2024)106 [arXiv:2401.08917 [hep-ph]].
- [55] S. Bisal and D. Das, Eur. Phys. J. C **84** (2024) no.6, 630 doi:10.1140/epjc/s10052-024-12984-3 [arXiv:2308.06558 [hep-ph]].
- [56] J. Cao, Y. He, L. Shang, W. Su and Y. Zhang, JHEP **08** (2016), 037 doi:10.1007/JHEP08(2016)037 [arXiv:1606.04416 [hep-ph]].
- [57] C. Beskidt, W. de Boer, D. I. Kazakov and S. Wayand, Phys. Lett. B **771** (2017), 611-618 doi:10.1016/j.physletb.2017.06.016 [arXiv:1703.01255 [hep-ph]].
- [58] W. Abdallah, A. Chatterjee and A. Datta, JHEP **1909**, 095 (2019) doi:10.1007/JHEP09(2019)095 [arXiv:1907.06270 [hep-ph]].
- [59] U. Ellwanger and A. M. Teixeira, JHEP **1410**, 113 (2014) doi:10.1007/JHEP10(2014)113 [arXiv:1406.7221 [hep-ph]].
- [60] U. Ellwanger, JHEP **1702**, 051 (2017) doi:10.1007/JHEP02(2017)051 [arXiv:1612.06574 [hep-ph]].

- [61] U. Ellwanger and C. Hugonie, Eur. Phys. J. C **78**, no. 9, 735 (2018) doi:10.1140/epjc/s10052-018-6204-3 [arXiv:1806.09478 [hep-ph]].
- [62] M. Guchait and A. Roy, Phys. Rev. D **102** no. 7, 075023 (2020) doi:10.1103/PhysRevD.102.075023 [arXiv:2005.05190 [hep-ph]].
- [63] G. Belanger, F. Boudjema, C. Hugonie, A. Pukhov and A. Semenov, JCAP **09** (2005), 001 doi:10.1088/1475-7516/2005/09/001 [arXiv:hep-ph/0505142 [hep-ph]].
- [64] J. F. Gunion, D. Hooper and B. McElrath, Phys. Rev. D **73** (2006), 015011 doi:10.1103/PhysRevD.73.015011 [arXiv:hep-ph/0509024 [hep-ph]].
- [65] W. Abdallah, A. Datta and S. Roy, [arXiv:2012.04026 [hep-ph]].
- [66] A. Datta, M. Guchait, A. Roy and S. Roy, JHEP **11** (2023), 081 doi:10.1007/JHEP11(2023)081 [arXiv:2211.05905 [hep-ph]].
- [67] R. Dermisek and J. F. Gunion, Phys. Rev. Lett. **95** (2005), 041801 doi:10.1103/PhysRevLett.95.041801 [arXiv:hep-ph/0502105 [hep-ph]].
- [68] R. Dermisek and J. F. Gunion, Phys. Rev. D **75** (2007), 075019 doi:10.1103/PhysRevD.75.075019 [arXiv:hep-ph/0611142 [hep-ph]].
- [69] D. G. Cerdeno, P. Ghosh and C. B. Park, JHEP **06** (2013), 031 doi:10.1007/JHEP06(2013)031 [arXiv:1301.1325 [hep-ph]].
- [70] N. D. Christensen, T. Han, Z. Liu and S. Su, JHEP **08** (2013), 019 doi:10.1007/JHEP08(2013)019 [arXiv:1303.2113 [hep-ph]].
- [71] D. G. Cerdeño, P. Ghosh, C. B. Park and M. Peiró, JHEP **02** (2014), 048 doi:10.1007/JHEP02(2014)048 [arXiv:1307.7601 [hep-ph]].
- [72] J. Cao, F. Ding, C. Han, J. M. Yang and J. Zhu, JHEP **11** (2013), 018 doi:10.1007/JHEP11(2013)018 [arXiv:1309.4939 [hep-ph]].
- [73] S. F. King, M. Mühlleitner, R. Nevzorov and K. Walz, Phys. Rev. D **90** (2014) no.9, 095014 doi:10.1103/PhysRevD.90.095014 [arXiv:1408.1120 [hep-ph]].
- [74] B. Dutta, Y. Gao and B. Shakya, Phys. Rev. D **91** (2015) no.3, 035016 doi:10.1103/PhysRevD.91.035016 [arXiv:1412.2774 [hep-ph]].
- [75] N. E. Bomark, S. Moretti and L. Roszkowski, J. Phys. G **43** (2016) no.10, 105003 doi:10.1088/0954-3899/43/10/105003 [arXiv:1503.04228 [hep-ph]].
- [76] U. Ellwanger and M. Rodriguez-Vazquez, JHEP **02** (2016), 096 doi:10.1007/JHEP02(2016)096 [arXiv:1512.04281 [hep-ph]].
- [77] E. Conte, B. Fuks, J. Guo, J. Li and A. G. Williams, JHEP **05** (2016), 100 doi:10.1007/JHEP05(2016)100 [arXiv:1604.05394 [hep-ph]].
- [78] M. Guchait and J. Kumar, Phys. Rev. D **95** (2017) no.3, 035036 doi:10.1103/PhysRevD.95.035036 [arXiv:1608.05693 [hep-ph]].
- [79] S. Baum, K. Freese, N. R. Shah and B. Shakya, Phys. Rev. D **95** (2017) no.11, 115036 doi:10.1103/PhysRevD.95.115036 [arXiv:1703.07800 [hep-ph]].
- [80] M. Guchait, A. H. Vijay and J. Kumar, JHEP **08** (2017), 122 doi:10.1007/JHEP08(2017)122 [arXiv:1705.06275 [hep-ph]].
- [81] U. Ellwanger and M. Rodriguez-Vazquez, JHEP **11** (2017), 008 doi:10.1007/JHEP11(2017)008 [arXiv:1707.08522 [hep-ph]].

- [82] D. Barducci, K. Mimasu, J. M. No, C. Vernieri and J. Zurita, JHEP **02** (2020), 002 doi:10.1007/JHEP02(2020)002 [arXiv:1910.08574 [hep-ph]].
- [83] M. Carena, J. Kozaczuk, Z. Liu, T. Ou, M. J. Ramsey-Musolf, J. Shelton, Y. Wang and K. P. Xie, LHEP **2023** (2023), 432 doi:10.31526/lhep.2023.432 [arXiv:2203.08206 [hep-ph]].
- [84] Y. Gershtein, S. Knapen and D. Redigolo, Phys. Lett. B **823** (2021), 136758 doi:10.1016/j.physletb.2021.136758 [arXiv:2012.07864 [hep-ph]].
- [85] M. Spira, Fortsch. Phys. **46** (1998), 203-284 doi:10.1002/(SICI)1521-3978(199804)46:3<203::AID-PROP203>3.0.CO;2-4 [arXiv:hep-ph/9705337 [hep-ph]].
- [86] M. W. Winkler, Phys. Rev. D **99** (2019) no.1, 015018 doi:10.1103/PhysRevD.99.015018 [arXiv:1809.01876 [hep-ph]].
- [87] M. Aaboud *et al.* [ATLAS], JHEP **06** (2018), 166 doi:10.1007/JHEP06(2018)166 [arXiv:1802.03388 [hep-ex]].
- [88] M. Aaboud *et al.* [ATLAS], Phys. Lett. B **782** (2018), 750-767 doi:10.1016/j.physletb.2018.06.011 [arXiv:1803.11145 [hep-ex]].
- [89] M. Aaboud *et al.* [ATLAS], JHEP **10** (2018), 031 doi:10.1007/JHEP10(2018)031 [arXiv:1806.07355 [hep-ex]].
- [90] M. Aaboud *et al.* [ATLAS], Phys. Lett. B **790** (2019), 1-21 doi:10.1016/j.physletb.2018.10.073 [arXiv:1807.00539 [hep-ex]].
- [91] G. Aad *et al.* [ATLAS], [arXiv:2005.12236 [hep-ex]].
- [92] A. M. Sirunyan *et al.* [CMS], JHEP **11** (2018), 018 doi:10.1007/JHEP11(2018)018 [arXiv:1805.04865 [hep-ex]].
- [93] A. M. Sirunyan *et al.* [CMS], Phys. Lett. B **795** (2019), 398-423 doi:10.1016/j.physletb.2019.06.021 [arXiv:1812.06359 [hep-ex]].
- [94] A. M. Sirunyan *et al.* [CMS], JHEP **08** (2020), 139 doi:10.1007/JHEP08(2020)139 [arXiv:2005.08694 [hep-ex]].
- [95] V. Khachatryan *et al.* [CMS], JHEP **10** (2017), 076 doi:10.1007/JHEP10(2017)076 [arXiv:1701.02032 [hep-ex]].
- [96] A. M. Sirunyan *et al.* [CMS], Phys. Lett. B **800** (2020), 135087 doi:10.1016/j.physletb.2019.135087 [arXiv:1907.07235 [hep-ex]].
- [97] G. Aad *et al.* [ATLAS], Phys. Rev. D **92** (2015) no.5, 052002 doi:10.1103/PhysRevD.92.052002 [arXiv:1505.01609 [hep-ex]].
- [98] A. M. Sirunyan *et al.* [CMS], JHEP **11** (2018), 018 doi:10.1007/JHEP11(2018)018 [arXiv:1805.04865 [hep-ex]].
- [99] A. M. Sirunyan *et al.* [CMS], JHEP **08** (2020), 139 doi:10.1007/JHEP08(2020)139 [arXiv:2005.08694 [hep-ex]].
- [100] [CMS], CMS-PAS-HIG-21-021.
- [101] [CMS], CMS-PAS-HIG-22-007.
- [102] A. M. Sirunyan *et al.* [CMS], Phys. Lett. B **778** (2018), 101-127 doi:10.1016/j.physletb.2018.01.001 [arXiv:1707.02909 [hep-ex]].

- [103] A. M. Sirunyan *et al.* [CMS], Phys. Lett. B **785** (2018), 462 doi:10.1016/j.physletb.2018.08.057 [arXiv:1805.10191 [hep-ex]].
- [104] M. Aaboud *et al.* [ATLAS], JHEP **06** (2018), 166 doi:10.1007/JHEP06(2018)166 [arXiv:1802.03388 [hep-ex]].
- [105] S. Chatrchyan *et al.* [CMS], Phys. Lett. B **726** (2013), 564-586 doi:10.1016/j.physletb.2013.09.009 [arXiv:1210.7619 [hep-ex]].
- [106] V. Khachatryan *et al.* [CMS], Phys. Lett. B **752** (2016), 146-168 doi:10.1016/j.physletb.2015.10.067 [arXiv:1506.00424 [hep-ex]].
- [107] A. M. Sirunyan *et al.* [CMS], Phys. Lett. B **796** (2019), 131-154 doi:10.1016/j.physletb.2019.07.013 [arXiv:1812.00380 [hep-ex]].
- [108] G. Aad *et al.* [ATLAS], JHEP **03** (2022), 041 doi:10.1007/JHEP03(2022)041 [arXiv:2110.13673 [hep-ex]].
- [109] M. Aaboud *et al.* [ATLAS], Phys. Lett. B **782**, 750-767 (2018) doi:10.1016/j.physletb.2018.06.011 [arXiv:1803.11145 [hep-ex]].
- [110] A. Tumasyan *et al.* [CMS], Eur. Phys. J. C **82** (2022) no.4, 290 doi:10.1140/epjc/s10052-022-10127-0 [arXiv:2111.01299 [hep-ex]].
- [111] G. Aad *et al.* [ATLAS], Phys. Rev. D **105** (2022) no.1, 012006 doi:10.1103/PhysRevD.105.012006 [arXiv:2110.00313 [hep-ex]].
- [112] A. M. Sirunyan *et al.* [CMS], Phys. Lett. B **795** (2019), 398-423 doi:10.1016/j.physletb.2019.06.021 [arXiv:1812.06359 [hep-ex]].
- [113] G. Aad *et al.* [ATLAS], [arXiv:2410.16781 [hep-ex]].
- [114] G. Aad *et al.* [ATLAS], Phys. Rev. D **110**, no.5, 052013 (2024) doi:10.1103/PhysRevD.110.052013 [arXiv:2407.01335 [hep-ex]].
- [115] G. Aad *et al.* [ATLAS], [arXiv:2405.04914 [hep-ex]].
- [116] [CMS], CMS-PAS-SUS-24-002.
- [117] [CMS], CMS-PAS-HIG-18-026.
- [118] A. Tumasyan *et al.* [CMS], JHEP **07**, 148 (2023) doi:10.1007/JHEP07(2023)148 [arXiv:2208.01469 [hep-ex]].
- [119] M. Aaboud *et al.* [ATLAS], JHEP **10** (2018), 031 doi:10.1007/JHEP10(2018)031 [arXiv:1806.07355 [hep-ex]].
- [120] G. Aad *et al.* [ATLAS], Phys. Rev. D **102** (2020) no.11, 112006 doi:10.1103/PhysRevD.102.112006 [arXiv:2005.12236 [hep-ex]].
- [121] [CMS], CMS-PAS-HIG-21-003.
- [122] B. Alves, CERN-THESIS-2024-262.
- [123] A. Liss *et al.* [ATLAS], [arXiv:1307.7292 [hep-ex]].
- [124] [CMS], [arXiv:1307.7135 [hep-ex]].
- [125] G. Aad *et al.* [ATLAS], Phys. Rev. D **101** (2020) no. 1, 012002 doi:10.1103/PhysRevD.101.012002 [arXiv:1909.02845 [hep-ex]].
- [126] A. M. Sirunyan *et al.* [CMS], Eur. Phys. J. C **79**, no. 5, 421 (2019) doi:10.1140/epjc/s10052-019-6909-y [arXiv:1809.10733 [hep-ex]].

- [127] A. Pierce, N. R. Shah and K. Freese, arXiv:1309.7351 [hep-ph].
- [128] L. Calibbi, J. M. Lindert, T. Ota and Y. Takanishi, JHEP **11** (2014), 106 doi:10.1007/JHEP11(2014)106 [arXiv:1410.5730 [hep-ph]].
- [129] M. Badziak, M. Olechowski and P. Szczerbiak, JHEP **1603**, 179 (2016) doi:10.1007/JHEP03(2016)179 [arXiv:1512.02472 [hep-ph]].
- [130] M. Badziak, M. Olechowski and P. Szczerbiak, JHEP **1707**, 050 (2017) doi:10.1007/JHEP07(2017)050 [arXiv:1705.00227 [hep-ph]].
- [131] C. Cheung, L. J. Hall, D. Pinner and J. T. Ruderman, JHEP **05** (2013), 100 doi:10.1007/JHEP05(2013)100 [arXiv:1211.4873 [hep-ph]].
- [132] G. Jungman, M. Kamionkowski and K. Griest, Phys. Rept. **267**, 195 (1996) doi:10.1016/0370-1573(95)00058-5 [hep-ph/9506380].
- [133] G. Belanger, F. Boudjema, A. Pukhov and A. Semenov, Comput. Phys. Commun. **180**, 747 (2009) doi:10.1016/j.cpc.2008.11.019 [arXiv:0803.2360 [hep-ph]].
- [134] M. Drees and M. M. Nojiri, Phys. Rev. D **48**, 3483 (1993) doi:10.1103/PhysRevD.48.3483 [hep-ph/9307208].
- [135] M. Drees and M. M. Nojiri, Phys. Rev. D **47**, 4226 (1993) doi:10.1103/PhysRevD.47.4226 [hep-ph/9210272].
- [136] Q. Riffard, F. Mayet, G. Bélanger, M. H. Genest and D. Santos, Phys. Rev. D **93** (2016) no.3, 035022 doi:10.1103/PhysRevD.93.035022 [arXiv:1602.01030 [hep-ph]].
- [137] J. Cao, Y. He, Y. Pan, Y. Yue, H. Zhou and P. Zhu, JHEP **2012**, 023 (2020) doi:10.1007/JHEP12(2020)023 [arXiv:1903.01124 [hep-ph]].
- [138] U. Ellwanger, J. F. Gunion and C. Hugonie, JHEP **02**, 066 (2005) doi:10.1088/1126-6708/2005/02/066 [arXiv:0406215 [hep-ph]].
- [139] U. Ellwanger and C. Hugonie, Comput. Phys. Commun. **175**, 290–303 (2006) doi:10.1016/j.cpc.2006.04.004 [arXiv:0508022 [hep-ph]].
- [140] F. Feroz, M. P. Hobson and M. Bridges, Mon. Not. Roy. Astron. Soc. **398**, 1601 (2009) doi:10.1111/j.1365-2966.2009.14548.x [arXiv:0809.3437 [astro-ph]].
- [141] F. Feroz, M. P. Hobson, E. Cameron and A. N. Pettitt, arXiv:1306.2144 [astro-ph.IM].
- [142] G. Degrassi, P. Slavich, Nucl. Phys. B **825**, 119–150 (2010) doi:10.1016/j.nuclphysb.2009.09.018 [arXiv:0907.4682 [hep-ph]].
- [143] S. Navas *et al.* [Particle Data Group], Phys. Rev. D **110** (2024) no.3, 030001 doi:10.1103/PhysRevD.110.030001
- [144] F. Domingo, U. Ellwanger, JHEP **12**, 090 (2007) doi:10.1088/1126-6708/2007/12/090 [arXiv:0710.3714 [hep-ph]].
- [145] Domingo, and Florian, Eur. Phys. J. C **76**, no. 8, 452 (2016) doi:10.1140/epjc/s10052-016-4298-z [arXiv:1512.02091 [hep-ph]].
- [146] S. Matsumoto, S. Mukhopadhyay and Y. L. S. Tsai, Phys. Rev. D **94** (2016) no.6, 065034 doi:10.1103/PhysRevD.94.065034 [arXiv:1604.02230 [hep-ph]].
- [147] G. Belanger, F. Boudjema, A. Pukhov *et al.* Comput. Phys. Commun. **174**, 577–604 (2006) doi:10.1016/j.cpc.2005.12.005 [arXiv:04052537 [hep-ph]].

- [148] G. Belanger, F. Boudjema, A. Pukhov *et al.* Comput. Phys. Commun. **176**, 367–382 (2007) doi:10.1016/j.cpc.2006.11.008 [arXiv:0607059 [hep-ph]].
- [149] G. Belanger, F. Boudjema, A. Pukhov *et al.* Comput. Phys. Commun. **185**, 960–985 (2014) doi:10.1016/j.cpc.2013.10.016 [arXiv:1305.0237 [hep-ph]].
- [150] G. Belanger, F. Boudjema, A. Goudelis *et al.* Comput. Phys. Commun. **231**, 173–186 (2018) doi:10.1016/j.cpc.2018.04.027 [arXiv:1801.03509 [hep-ph]].
- [151] D. P. Aguillard *et al.* [Muon g-2], Phys. Rev. Lett. **131** (2023) no.16, 161802 doi:10.1103/PhysRevLett.131.161802 [arXiv:2308.06230 [hep-ex]].
- [152] T. Aoyama, N. Asmussen, M. Benayoun, J. Bijnens, T. Blum, M. Bruno, I. Caprini, C. M. Carloni Calame, M. Cè and G. Colangelo, *et al.* Phys. Rept. **887** (2020), 1-166 doi:10.1016/j.physrep.2020.07.006 [arXiv:2006.04822 [hep-ph]].
- [153] P. Stoffer, G. Colangelo and M. Hoferichter, JINST **18** (2023) no.10, C10021 doi:10.1088/1748-0221/18/10/C10021 [arXiv:2308.04217 [hep-ph]].
- [154] N. Bray-Ali, [arXiv:2308.11650 [hep-ph]].
- [155] G. Venanzoni [Muon g-2], PoS **EPS-HEP2023** (2024), 037 doi:10.22323/1.449.0037 [arXiv:2311.08282 [hep-ex]].
- [156] S. Kuberski, PoS **LATTICE2023** (2024), 125 doi:10.22323/1.453.0125 [arXiv:2312.13753 [hep-lat]].
- [157] D. P. Aguillard *et al.* [Muon g-2], Phys. Rev. D **110** (2024) no.3, 032009 doi:10.1103/PhysRevD.110.032009 [arXiv:2402.15410 [hep-ex]].
- [158] S. Borsanyi, Z. Fodor, J. N. Guenther, C. Hoelbling, S. D. Katz, L. Lellouch, T. Lippert, K. Miura, L. Parato and K. K. Szabo, *et al.* Nature **593** (2021) no.7857, 51-55 doi:10.1038/s41586-021-03418-1 [arXiv:2002.12347 [hep-lat]].
- [159] M. Davier, Z. Fodor, A. Gerardin, L. Lellouch, B. Malaescu, F. M. Stokes, K. K. Szabo, B. C. Toth, L. Varnhorst and Z. Zhang, Phys. Rev. D **109** (2024) no.7, 076019 doi:10.1103/PhysRevD.109.076019 [arXiv:2308.04221 [hep-ph]].
- [160] F. V. Ignatov *et al.* [CMD-3], Phys. Rev. D **109** (2024) no.11, 112002 doi:10.1103/PhysRevD.109.112002 [arXiv:2302.08834 [hep-ex]].
- [161] F. V. Ignatov *et al.* [CMD-3], Phys. Rev. Lett. **132** (2024) no.23, 231903 doi:10.1103/PhysRevLett.132.231903 [arXiv:2309.12910 [hep-ex]].
- [162] P. Athron, C. Balázs, D. H. J. Jacob, W. Kotlarski, D. Stöckinger and H. Stöckinger-Kim, JHEP **09** (2021), 080 doi:10.1007/JHEP09(2021)080 [arXiv:2104.03691 [hep-ph]].
- [163] M. Lindner, M. Platscher and F. S. Queiroz, Phys. Rept. **731** (2018), 1-82 doi:10.1016/j.physrep.2017.12.001 [arXiv:1610.06587 [hep-ph]].
- [164] P. Bechtle, S. Heinemeyer, O. Stål, T. Stefaniak and G. Weiglein, Eur. Phys. J. C **74** (2014) no.2, 2711 doi:10.1140/epjc/s10052-013-2711-4 [arXiv:1305.1933 [hep-ph]].
- [165] O. Stål and T. Stefaniak, PoS **EPS-HEP2013** (2013), 314 doi:10.22323/1.180.0314 [arXiv:1310.4039 [hep-ph]].
- [166] P. Bechtle, S. Heinemeyer, O. Stål, T. Stefaniak and G. Weiglein, JHEP **11** (2014), 039 doi:10.1007/JHEP11(2014)039 [arXiv:1403.1582 [hep-ph]].

- [167] P. Bechtle, S. Heinemeyer, T. Klingl, T. Stefaniak, G. Weiglein and J. Wittbrodt, Eur. Phys. J. C **81** (2021) no.2, 145 doi:10.1140/epjc/s10052-021-08942-y [arXiv:2012.09197 [hep-ph]].
- [168] P. Bechtle, O. Brein, S. Heinemeyer, G. Weiglein and K. E. Williams, Comput. Phys. Commun. **181** (2010), 138-167 doi:10.1016/j.cpc.2009.09.003 [arXiv:0811.4169 [hep-ph]].
- [169] P. Bechtle, O. Brein, S. Heinemeyer, G. Weiglein and K. E. Williams, Comput. Phys. Commun. **182** (2011), 2605-2631 doi:10.1016/j.cpc.2011.07.015 [arXiv:1102.1898 [hep-ph]].
- [170] P. Bechtle, O. Brein, S. Heinemeyer, O. Stål, T. Stefaniak, G. Weiglein and K. Williams, PoS **CHARGED2012** (2012), 024 doi:10.22323/1.156.0024 [arXiv:1301.2345 [hep-ph]].
- [171] P. Bechtle, O. Brein, S. Heinemeyer, O. Stål, T. Stefaniak, G. Weiglein and K. E. Williams, Eur. Phys. J. C **74** (2014) no.3, 2693 doi:10.1140/epjc/s10052-013-2693-2 [arXiv:1311.0055 [hep-ph]].
- [172] P. Bechtle, D. Dercks, S. Heinemeyer, T. Klingl, T. Stefaniak, G. Weiglein and J. Wittbrodt, Eur. Phys. J. C **80** (2020) no.12, 1211 doi:10.1140/epjc/s10052-020-08557-9 [arXiv:2006.06007 [hep-ph]].
- [173] D. J. Miller, R. Nevezorov and P. M. Zerwas, Nucl. Phys. B **681** (2004), 3-30 doi:10.1016/j.nuclphysb.2003.12.021 [arXiv:hep-ph/0304049 [hep-ph]].
- [174] J. L. Hintze and R. D. Nelson, *Violin plots: a box plot-density trace synergism*, *The American Statistician* **52** (1998) 181.
- [175] M. L. Ahnen *et al.* [MAGIC and Fermi-LAT], JCAP **02**, 039 (2016) doi:10.1088/1475-7516/2016/02/039 [arXiv:1601.06590 [astro-ph.HE]].
- [176] M. Ackermann *et al.* [Fermi-LAT], Phys. Rev. Lett. **115**, no.23, 231301 (2015) doi:10.1103/PhysRevLett.115.231301 [arXiv:1503.02641 [astro-ph.HE]].
- [177] A. Albert *et al.* [Fermi-LAT and DES], Astrophys. J. **834** (2017) no.2, 110 doi:10.3847/1538-4357/834/2/110 [arXiv:1611.03184 [astro-ph.HE]].
- [178] S. Baum, L. Visinelli, K. Freese and P. Stengel, Phys. Rev. D **95** (2017) no.4, 043007 doi:10.1103/PhysRevD.95.043007 [arXiv:1611.09665 [astro-ph.CO]].
- [179] J. D. Zornoza and C. Toennis, J. Phys. Conf. Ser. **888** (2017) no.1, 012206 doi:10.1088/1742-6596/888/1/012206 [arXiv:1611.02555 [astro-ph.HE]].
- [180] M. G. Aartsen *et al.* [IceCube], JCAP **04** (2016), 022 doi:10.1088/1475-7516/2016/04/022 [arXiv:1601.00653 [hep-ph]].
- [181] Khosa, C. K., Kraml, Sabine, Lessa, Andre, Neuhuber, Philipp, Waltenberger and Wolfgang, doi:10.31526/lhep.2020.158 [arXiv:2005.00555 [hep-ph]].
- [182] G. Aad *et al.* [ATLAS], JHEP **04** (2014), 169 doi:10.1007/JHEP04(2014)169 [arXiv:1402.7029 [hep-ex]].
- [183] A. M. Sirunyan *et al.* [CMS], JHEP **03** (2018), 076 doi:10.1007/s13130-018-7845-2 [arXiv:1709.08908 [hep-ex]].
- [184] A. M. Sirunyan *et al.* [CMS], JHEP **03** (2018), 166 doi:10.1007/JHEP03(2018)166 [arXiv:1709.05406 [hep-ex]].
- [185] A. M. Sirunyan *et al.* [CMS], Phys. Lett. B **779** (2018), 166-190 doi:10.1016/j.physletb.2017.12.069 [arXiv:1709.00384 [hep-ex]].

- [186] A. M. Sirunyan *et al.* [CMS], Phys. Lett. B **782** (2018), 440-467
doi:10.1016/j.physletb.2018.05.062 [arXiv:1801.01846 [hep-ex]].
- [187] A. M. Sirunyan *et al.* [CMS], JHEP **03** (2018), 160 doi:10.1007/JHEP03(2018)160
[arXiv:1801.03957 [hep-ex]].
- [188] A. M. Sirunyan *et al.* [CMS], Phys. Lett. B **790** (2019), 140-166
doi:10.1016/j.physletb.2019.01.005 [arXiv:1806.05264 [hep-ex]].
- [189] A. M. Sirunyan *et al.* [CMS], JHEP **11** (2018), 079 doi:10.1007/JHEP11(2018)079
[arXiv:1807.07799 [hep-ex]].
- [190] M. Aaboud *et al.* [ATLAS], Eur. Phys. J. C **78** (2018) no.12, 995
doi:10.1140/epjc/s10052-018-6423-7 [arXiv:1803.02762 [hep-ex]].
- [191] M. Aaboud *et al.* [ATLAS], Phys. Rev. D **98** (2018) no.9, 092012
doi:10.1103/PhysRevD.98.092012 [arXiv:1806.02293 [hep-ex]].
- [192] M. Aaboud *et al.* [ATLAS], Phys. Rev. D **100** (2019) no.1, 012006
doi:10.1103/PhysRevD.100.012006 [arXiv:1812.09432 [hep-ex]].
- [193] A. M. Sirunyan *et al.* [CMS], JHEP **04** (2021), 123 doi:10.1007/JHEP04(2021)123
[arXiv:2012.08600 [hep-ex]].
- [194] A. Tumasyan *et al.* [CMS], JHEP **05** (2022), 014 doi:10.1007/JHEP05(2022)014
[arXiv:2201.04206 [hep-ex]].
- [195] A. Tumasyan *et al.* [CMS], Phys. Lett. B **842** (2023), 137460
doi:10.1016/j.physletb.2022.137460 [arXiv:2205.09597 [hep-ex]].
- [196] G. Aad *et al.* [ATLAS], Eur. Phys. J. C **80** (2020) no.2, 123
doi:10.1140/epjc/s10052-019-7594-6 [arXiv:1908.08215 [hep-ex]].
- [197] G. Aad *et al.* [ATLAS], Eur. Phys. J. C **80** (2020) no.8, 691
doi:10.1140/epjc/s10052-020-8050-3 [arXiv:1909.09226 [hep-ex]].
- [198] G. Aad *et al.* [ATLAS], Phys. Rev. D **101** (2020) no.5, 052005
doi:10.1103/PhysRevD.101.052005 [arXiv:1911.12606 [hep-ex]].
- [199] G. Aad *et al.* [ATLAS], Phys. Rev. D **101** (2020) no.7, 072001
doi:10.1103/PhysRevD.101.072001 [arXiv:1912.08479 [hep-ex]].
- [200] G. Aad *et al.* [ATLAS], Eur. Phys. J. C **81** (2021) no.12, 1118
doi:10.1140/epjc/s10052-021-09749-7 [arXiv:2106.01676 [hep-ex]].
- [201] G. Aad *et al.* [ATLAS], Phys. Rev. D **104** (2021) no.11, 112010
doi:10.1103/PhysRevD.104.112010 [arXiv:2108.07586 [hep-ex]].
- [202] G. Aad *et al.* [ATLAS], Eur. Phys. J. C **83** (2023) no.6, 515
doi:10.1140/epjc/s10052-023-11434-w [arXiv:2204.13072 [hep-ex]].
- [203] G. Aad *et al.* [ATLAS], JHEP **06** (2023), 031 doi:10.1007/JHEP06(2023)031
[arXiv:2209.13935 [hep-ex]].
- [204] S. Amoroso *et al.* [LHC-TeV MW Working Group], Eur. Phys. J. C **84**, no.5, 451 (2024)
doi:10.1140/epjc/s10052-024-12532-z [arXiv:2308.09417 [hep-ex]].
- [205] T. J. Hou, K. Xie, J. Gao, S. Dulat, M. Guzzi, T. J. Hobbs, J. Huston, P. Nadolsky,
J. Pumplin and C. Schmidt, *et al.* [arXiv:1908.11394 [hep-ph]].

- [206] E. Bagnaschi, M. Chakraborti, S. Heinemeyer, I. Saha and G. Weiglein, Eur. Phys. J. C **82**, no.5, 474 (2022) doi:10.1140/epjc/s10052-022-10402-0 [arXiv:2203.15710 [hep-ph]].
- [207] T. P. Tang, M. Abdughani, L. Feng, Y. L. S. Tsai, J. Wu and Y. Z. Fan, Sci. China Phys. Mech. Astron. **66**, no.3, 239512 (2023) doi:10.1007/s11433-022-2046-y [arXiv:2204.04356 [hep-ph]].
- [208] F. Domingo, U. Ellwanger and C. Hugonie, Eur. Phys. J. C **82**, no.11, 1074 (2022) doi:10.1140/epjc/s10052-022-11059-5 [arXiv:2209.03863 [hep-ph]].
- [209] D. Curtin, R. Essig, S. Gori, P. Jaiswal, A. Katz, T. Liu, Z. Liu, D. McKeen, J. Shelton and M. Strassler, *et al.* Phys. Rev. D **90** (2014) no.7, 075004 doi:10.1103/PhysRevD.90.075004 [arXiv:1312.4992 [hep-ph]].
- [210] A. Abada *et al.* [FCC], Eur. Phys. J. C **79** (2019) no.6, 474 doi:10.1140/epjc/s10052-019-6904-3
- [211] J. B. Guimarães da Costa *et al.* [CEPC Study Group], [arXiv:1811.10545 [hep-ex]].
- [212] A. Abada *et al.* [FCC], Eur. Phys. J. ST **228** (2019) no.4, 755-1107 doi:10.1140/epjst/e2019-900087-0
- [213] A. Abada *et al.* [FCC], Eur. Phys. J. ST **228** (2019) no.2, 261-623 doi:10.1140/epjst/e2019-900045-4
- [214] M. Cepeda, S. Gori, V. M. Ootschoorn and J. Shelton, doi:10.1146/annurev-nucl-102319-024147 [arXiv:2111.12751 [hep-ph]].
- [215] D. de Florian *et al.* [LHC Higgs Cross Section Working Group], doi:10.23731/CYRM-2017-002 [arXiv:1610.07922 [hep-ph]].
- [216] M. Cepeda, S. Gori, P. Ilten, M. Kado, F. Riva, R. Abdul Khalek, A. Aboubrahim, J. Alimena, S. Alioli and A. Alves, *et al.* CERN Yellow Rep. Monogr. **7** (2019), 221-584 doi:10.23731/CYRM-2019-007.221 [arXiv:1902.00134 [hep-ph]].
- [217] Z. Liu, L. T. Wang and H. Zhang, Chin. Phys. C **41** (2017) no.6, 063102 doi:10.1088/1674-1137/41/6/063102 [arXiv:1612.09284 [hep-ph]].